Engineering with Computers (2021) 37:1181–1204
https://doi.org/10.1007/s00366-019-00878-y

ORIGINAL ARTICLE

Prediction of quality characteristics of laser drilled holes using artificial intelligence techniques

Suman Chatterjee[1] · Siba Sankar Mahapatra[1] · Vijay Bharadwaj[2] · Brahma N. Upadhyay[2] · Khushvinder S. Bindra[2]

Received: 8 July 2019 / Accepted: 18 October 2019 / Published online: 7 November 2019

Abstract
Micro-drilling using lasers finds widespread industrial applications in aerospace, automobile, and bio-medical sectors for obtaining holes of precise geometric quality with crack-free surfaces. In order to achieve holes of desired quality on hard-to-machine materials in an economical manner, computational intelligence approaches are being used for accurate prediction of performance measures in drilling process. In the present study, pulsed millisecond Nd:YAG laser is used for micro drilling of titanium alloy and stainless steel under identical machining conditions by varying the process parameters such as current, pulse width, pulse frequency, and gas pressure at different levels. Artificial intelligence techniques such as adaptive neuro-fuzzy inference system (ANFIS) and multi gene genetic programming (MGGP) are used to predict the performance measures, e.g. circularity at entry and exit, heat affected zone, spatter area and taper. Seventy percent of the experimental data constitutes the training set whereas remaining thirty percent data is used as testing set. The results indicate that root mean square error (RMSE) for testing data set lies in the range of 8.17–24.17% and 4.04–18.34% for ANFIS model MGGP model, respectively, when drilling is carried out on titanium alloy work piece. Similarly, RMSE for testing data set lies in the range of 13.08–20.45% and 6.35–10.74% for ANFIS and MGGP model, respectively, for stainless steel work piece. Comparative analysis of both ANFIS and MGGP models suggests that MGGP predicts the performance measures in a superior manner in laser drilling operation and can be potentially applied for accurate prediction of machining output.

Keywords Artificial intelligence · Laser drilling · Genetic programming · ANFIS · Stainless steel · Surface cracks · Ti6Al4V

1 Introduction

Lasers find wide range of applications in various sectors such as manufacturing, aerospace and aviation, automobile, electrical and electronics and medical sectors. Lasers are used in various material processing techniques like laser peening, laser forming, laser welding, laser cutting, laser milling, laser drilling and laser-assisted machining due to its benefits such as less machining time, high precision and repeatability of the processes. Among all laser beam machining processes, laser drilling has engrossed attention recently [1, 2]. Due to the short interface time between the materials and laser, millisecond laser and ultrafast lasers have been considered as the preeminent techniques for drilling of brittle and hard-to-machine materials such as Inconel, titanium alloys and stainless steels. Stainless steel and titanium alloys are widely used in various fields such as electrical and electronics, petrochemical, shipping, aviation and aerospace, automobile and manufacturing industries and medical science due to their favorable mechanical, thermal and chemical properties. However, laser drilling of such materials is difficult because it induces various defects viz. micro-cracks, spatter, heat-affected zone, circularity and taper. Extensive research works have been carried out for optimization of process parameters so as to improve the performance measures, e.g. geometric and surface quality and heat-induced characteristics of laser-drilled holes [3–5]. Since laser drilling process is a costly process, development of such defects causes loss in economy. To overcome such difficulties, it is imperative to develop predictive models

✉ Suman Chatterjee
mrsumanmech@gmail.com

[1] Department of Mechanical Engineering, National Institute of Technology, Rourkela 769008, India

[2] Laser Development and Industrial Applications Division, Raja Ramanna Centre for Advanced Technology, Indore 452013, India

based on artificial intelligence techniques embedded with meta-heuristic approaches for optimization of the quality characteristics.

Casalino [5] have presented potential application of computational intelligence techniques for prediction, modeling and optimization of various laser material processing methods. The study shows that computational intelligence algorithms are capable of determining the hidden knowledge from experimental data to make complex decisions without human intervention. Hajihassani et al. [6] have proposed artificial and meta-heuristic approaches for prediction and optimization of the construction processes. Parandoush and Hossain [7] have presented a detailed study on scope for prediction and optimization of machining responses during laser beam machining (LBM) using artificial intelligence techniques such as artificial neural network, genetic algorithm and fuzzy expert system. The study states that artificial intelligence techniques have good potential to understand the machining behavior with less human effort. As laser drilling, especially micro- and nano-scale machining process, is a complicated process, prediction of process behavior makes the way to understand the difficult process behavior for the practitioners. Vijayaraghavan et al. [8] have proposed genetic programming (GP) and artificial neural network (ANN) approach for predicting the quality characteristics during drilling of grapheme sheets. The study shows that results obtained using genetic programming have good agreement with the experimental results as compared to ANN approach. Sibalija et al. [9] have conducted laser drilling on nickel-based super alloys having thickness of 1.2 mm using Nd:YAG laser varying two process parameters such as pulse frequency and pulse duration to analyze the seven drilling responses. Sibalija et al. [9] have proposed artificial intelligence method like artificial neural network technique and statistical approach such as Taguchi's quality loss function, gray relation analysis (GRA) and principal component analysis (PCA) for prediction and optimization of the seven process outputs in laser drilling of nimonic alloy. The results suggest that prediction capability of ANN is superior to statistical methods. Bello et al. [10] have reported that artificial intelligence techniques are potentially suitable to be applied in the field of drilling. Gill and Singh [11] have proposed adaptive neuro-fuzzy inference system (ANFIS) to develop a predictive model for estimation of material removal rate (MRR) during drilling of ceramic alloys. Pérez et al. [12] have adopted adaptive neuro-fuzzy inference system for modeling of quality measures in laser surface treatment process.

As drilling is a complex process, researchers have proposed various computational approaches such as regression analysis, support vector machine (SVM) and artificial neural network [13] to achieve better prediction capability. Garg et al. [13] have proposed a predictive model based on multi gene genetic programming (MGGP) to estimate the burr height in drilling of AISI 316L and compared the results with regression analysis, support vector machine and artificial neural network. The results suggest that MGGP possesses reasonable potential to be treated as a good predictive model. Abhishek et al. [14] have demonstrated prediction capability of genetic programming (GP) and ANFIS models in drilling of composites. Abidin et al. [15] have used various soft computing approaches to obtain optimum parametric setting for estimating drilling path in various drilling methods.

Desai and Shaikh [16] have conducted a comparative study on prediction capability of different predictive models such as artificial neural network, semi-analytical technique and genetic programming while measuring the depth of cut in laser micro milling of thermoplastics. The study shows that GP produces less prediction error as compared to other models although all the techniques have reasonable accuracy in predicting the depth of cut. To predict the performance measures during turning of stainless steel, Garg and Tai [17] have preferred computational techniques using fuzzy logic, support vector regression, regression analysis, artificial neural network and genetic programming over physics-based models for predicting the performance measures. It is stated that genetic programming is quite robust in prediction over other methodologies. González et al. [18] have proposed an ANN model for predicting the dimensional error during ball end milling process. Khandelwal et al. [19] have proposed two different predictive models such as non-linear multi regression model and genetic programming for the estimation of properties of rock and suggest the superiority of the GP model over non-linear multi regression model. Asiltürk and Çunkaş [20] have used artificial neural network and multiple regression analysis for prediction of surface roughness during turning of stainless steel. It is observed that artificial neural network predicts the output with greater accuracy as compared to statistical method.

Extensive literature survey indicates that prior works are limited to identify the significant process parameters and their effect on the performance measures, predict quality characteristics and optimize the process parameters using statistical, computational and meta-heuristic approaches in different machining processes. However, potential of application of computational intelligence and meta-heuristic approaches is hardly explored for prediction and optimization of performance measures in laser drilling operation. With growth in miniaturization of existing products, there is rapid demand in production of micro machined products with high geometric quality and crack-free surfaces. To achieve the desired quality holes for hard-to-machine materials in an economical manner, it is imperative that computational intelligence approaches can predict the process behavior in an effective manner. The purpose of the present

study was to propose a model to predict quality characteristics of micro holes made on hard-to-machine materials like AISI 316 and Ti6Al4V using pulsed Nd:YAG laser. Pulsed millisecond Nd:YAG laser is used for micro drilling of Ti6Al4V and AISI 316 under identical machining conditions (same parametric setting) varying the process parameters such as current, pulse width, pulse frequency and gas pressure at three different levels to determine the performance measures, e.g. circularity at entry and exit, heat affected zone, spatter area and taper. Artificial intelligence techniques such as adaptive neuro-fuzzy inference system (ANFIS) and multi-gene genetic programming (MGGP), are used not only to predict the performance measures but also to analyze the variation of performance measures with the change in process parameters beyond experimental domain once the proposed models are converged.

2 Methodology

Artificial and computational intelligence generally involves use of computer algorithms to capture the hidden knowledge from data and uses them for training "intelligent machine" to make decisions without human intervention [5]. As simulation is becoming more prevalent from product design and planning manufacturing operations point of view, laser material processing can also be benefit from the computer generating knowledge through soft computing [5]. Laouissi et al. [21] have proposed statistical approach using response surface methodology (RSM) and artificial intelligence like ANN for predicting the machining outputs during turning of EN-GJL-250 cast iron. Laouissi et al. [21] have also optimized machining outputs using genetic algorithm (GA) after prediction of machining outputs using RSM and ANN. The study shows the scope for implementation of heuristic approach for optimization after prediction through statistical and artificial intelligence techniques during high-speed machining. Bustillo and Correa [22] have proposed artificial intelligence method for predicting surface roughness in high-speed machining process. Bayesian network approach is used to predict the surface roughness of the work piece in dry and lubricating (using minimum quantity lubrication) conditions and the predicted results are quite closer to experimented values.

2.1 Adaptive neuro-fuzzy inference system (ANFIS)

Adaptive neuro-fuzzy inference system is widely applied for predicting quality characteristics in the field of manufacturing engineering. Gholami et al. [23] have proposed a hybrid technique using meta-heuristic approach like particle swarm optimization algorithm embedded adaptive neuro-fuzzy inference system for prediction and optimization of threshold bank profile shape using digital laser. The study suggests that results obtained using meta-heuristic approach embedded with predictive technique have less uncertainty in nature. Petković et al. [24] have adopted adaptive neuro-fuzzy inference system to develop a predictive model to forecast the heat-affected zone (HAZ) during laser cutting of glass fiber reinforced plastic. Abdulshahed et al. [25] and Abdulshahed et al. [26] have proposed adaptive neuro-fuzzy inference system to predict the thermal error developed in the machine tool during computerized numerical control (CNC) milling process. Al-Ghamdi and Taylan [27] have adopted an adaptive neuro fuzzy inference system for predicting the material removal rate in electrical discharge machining (EDM) process. Sohrabpoor [28] have proposed a response model based on ANFIS and meta-heuristic approach known as imperialist competitive algorithm (ICA) to optimize process parameters in laser cladding process. Sohrabpoor [29] have adopted ANFIS to predict the performance of graphene-metal alloys in laser cladding process.

Adaptive neuro fuzzy inference system (ANFIS) is a mixed pattern of two artificial intelligence techniques known as artificial neural network (ANN) and fuzzy inference system (FIS). Fuzzy logic and neural network are two complementary techniques. Neural network has the capability of learning from both data and feedback without getting involved in understanding the pattern in the data sets. But, fuzzy logic model patterns are easy to comprehend because they use linguistic terms in the form of IF–THEN rules. A neural network with their learning proficiencies can be used to learn the fuzzy decision rules; this helps in development of a hybrid intelligent system network.

The fuzzy system provides expert knowledge to be used by the neural network. ANFIS consists of five layers and each layer consists of some nodes like artificial neural network (ANN). Figure 1 indicates the adaptive network structure for ANFIS. The structure for adaptive neuro-fuzzy inference system is characterized as follows. The details of each layer have been already discussed in the past literature [11, 23–28, 30]:

- Layer 1 consists of fuzzification layer.
- Layer 2 is known as product layer.
- Layer 3 is called as normalized layer.
- Layer 4 is the defuzzification layer.
- Layer 5 is known as output layer.

2.2 Multi gene genetic programming (MGGP)

In the present study, multi gene genetic programming is proposed for development of a predictive model for prediction of quality measures in laser drilling process. Genetic programming (GP) is first introduced by Koza in early 1990s [31–33]. GP is probably the most general approach

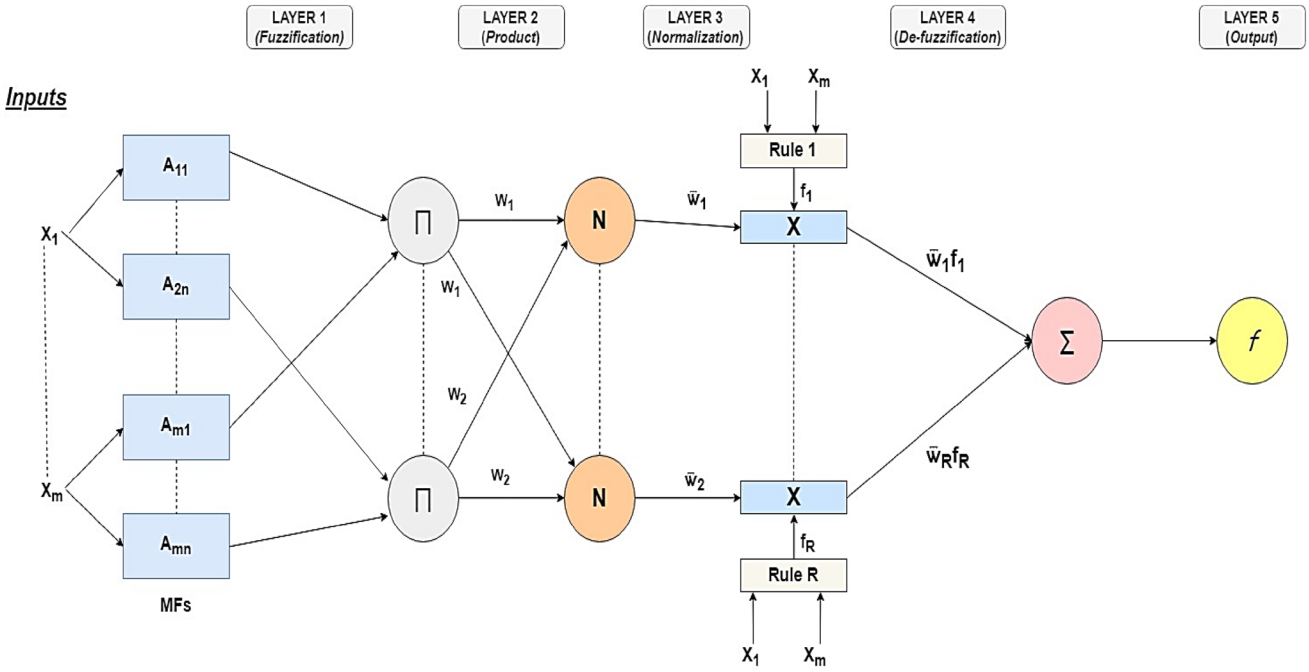

Fig. 1 Basic network structure for ANFIS

of evolutionary computation methods and applied for simple and complex systems in all aspects of engineering problem [34]. Sharma et al. [35] have proposed Taguchi method embedded with genetic programming method for prediction of compaction strength in powder metallurgy (PM) process. Panda et al. [36] have used genetic programming-based model for predicting the bead dimensions in wire and arc additive manufacturing. Kok et al. [37] have proposed a predictive model for estimation of surface roughness using genetic expression programming. Garg and Lam [38] have proposed multi gene genetic programming approach to develop an empirical relationship between input parameters and performance measures such as surface roughness, tool life and power consumption while turning of stainless steel and aluminum alloy. Brezocnik et al. [39] have proposed genetic programming to develop a model for prediction of surface roughness of drilled holes produced through milling process.

Multi gene genetic programming is a robust modified version of genetic programming. It successfully integrates the model structure selection ability of the standard GP with the parameter estimation power of classical regression [34]. Instead of complex rules and mathematical routines, MGGP is able to learn the key information patterns within the multidimensional information domain with high speed [34]. The steps (pseudo code) for the MGGP have been illustrated as follows (Table 1). The more detailed

Table 1 Steps (pseudo-code) involved in MGGP [13]

BEGIN
Step I: Formulation of problem
Step II: Multi gene genetic programming (MGGP) algorithm
Begin
II-a: Establishing parameters for the algorithm e.g. terminal and function set, number of generations, population size, genetic operators rate and maximum number of genes
II-b: Initiate initial population size for the genes
II-c: Models are formed by combining set of genes using least square method
II-d: Calculate performance of models based on root mean square error (RMSE)
II-e: Apply genetic operations and form the new population
III-f: Cross-check the model performance against the termination criterion and if not satisfied
GOTO Step II-e
End:
END:

explanations about multi gene genetic programming (MGGP) are available in literature [13, 34, 36, 38].

3 Materials and methods

3.1 Materials

Laser beam micro-drilling is performed on commercially available stainless steel (AISI 316) and titanium alloy (Ti6Al4V) having dimension of $50 \times 50 \times 0.45$ mm^3. The materials have been procured from Manohar Metal Corporation (Mumbai, India) for laser beam drilling purpose. The selection of materials and thickness is based on applications, commercial availability and economic reasons. Field emission scanning electron microscopy with energy dispersive spectroscopy (FESEM-EDS) has been performed to obtain the weight percentage of constituents present in the work piece and confirms the chemical composition of the as received work piece of AISI 316and Ti6Al4V. Figures 2 and 3 indicate the weight percentage of constituents available in work piece 1 (AISI 316 stainless steel) and work piece 2 (Ti6Al4V titanium alloy), respectively, and confirms the material composition of the available materials.

3.2 Methods

Laser beam micro drilling is a thermal ablation process in which high-intensity energy beam is focused at a point. This laser guided beam helps in melting and evaporation of molten material from the focus zone of the work piece. The molten materials from the drilled area are flushed away with the help of assistant gas pressure. Since laser guided beam can be focused on a very small diameter with high accuracy, it helps in attaining precise micro-drilled holes [5]. In the present study, laser drilling is performed on a

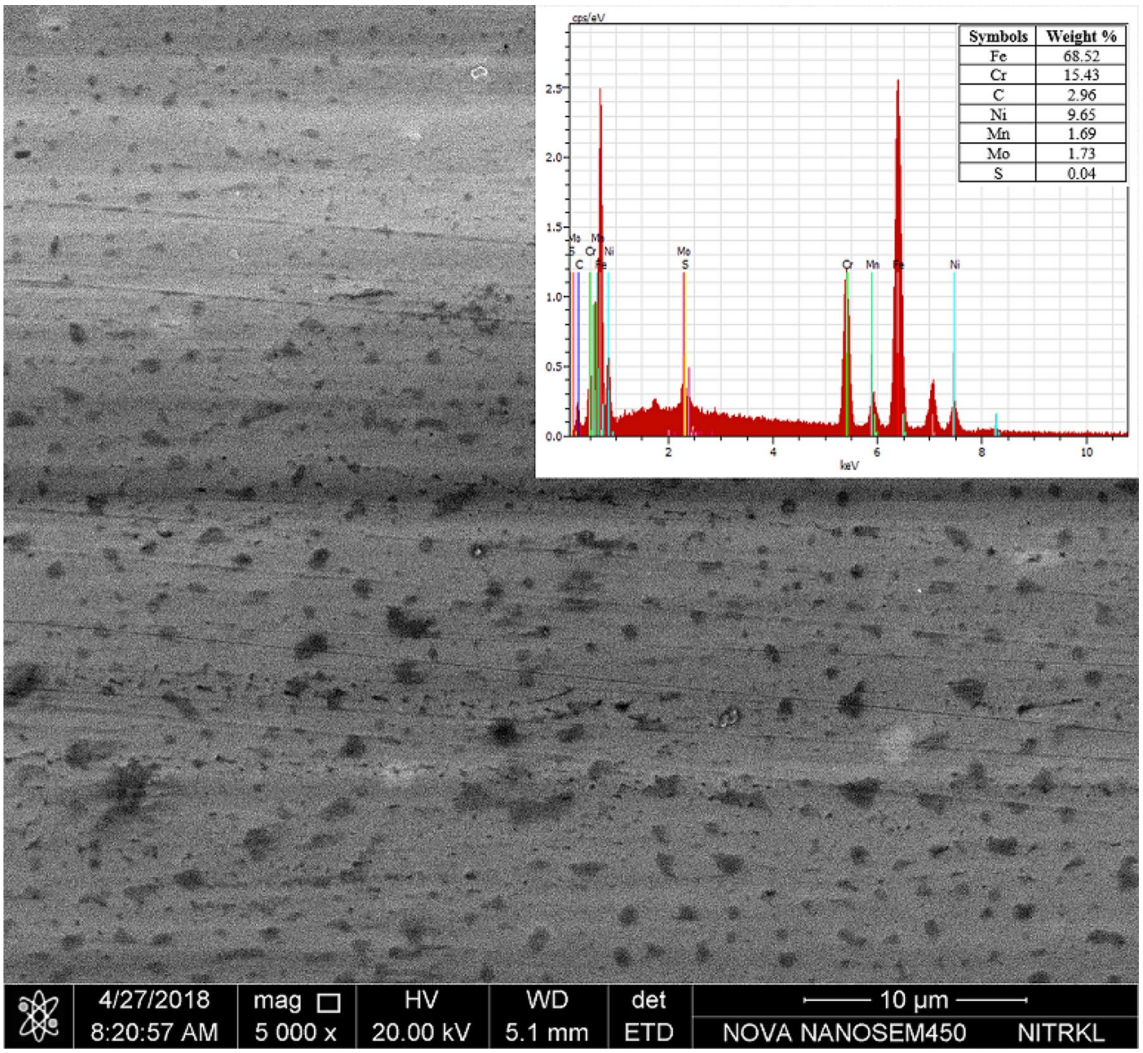

Fig. 2 FESEM-EDS graph for work piece 2 (AISI 316 as received)

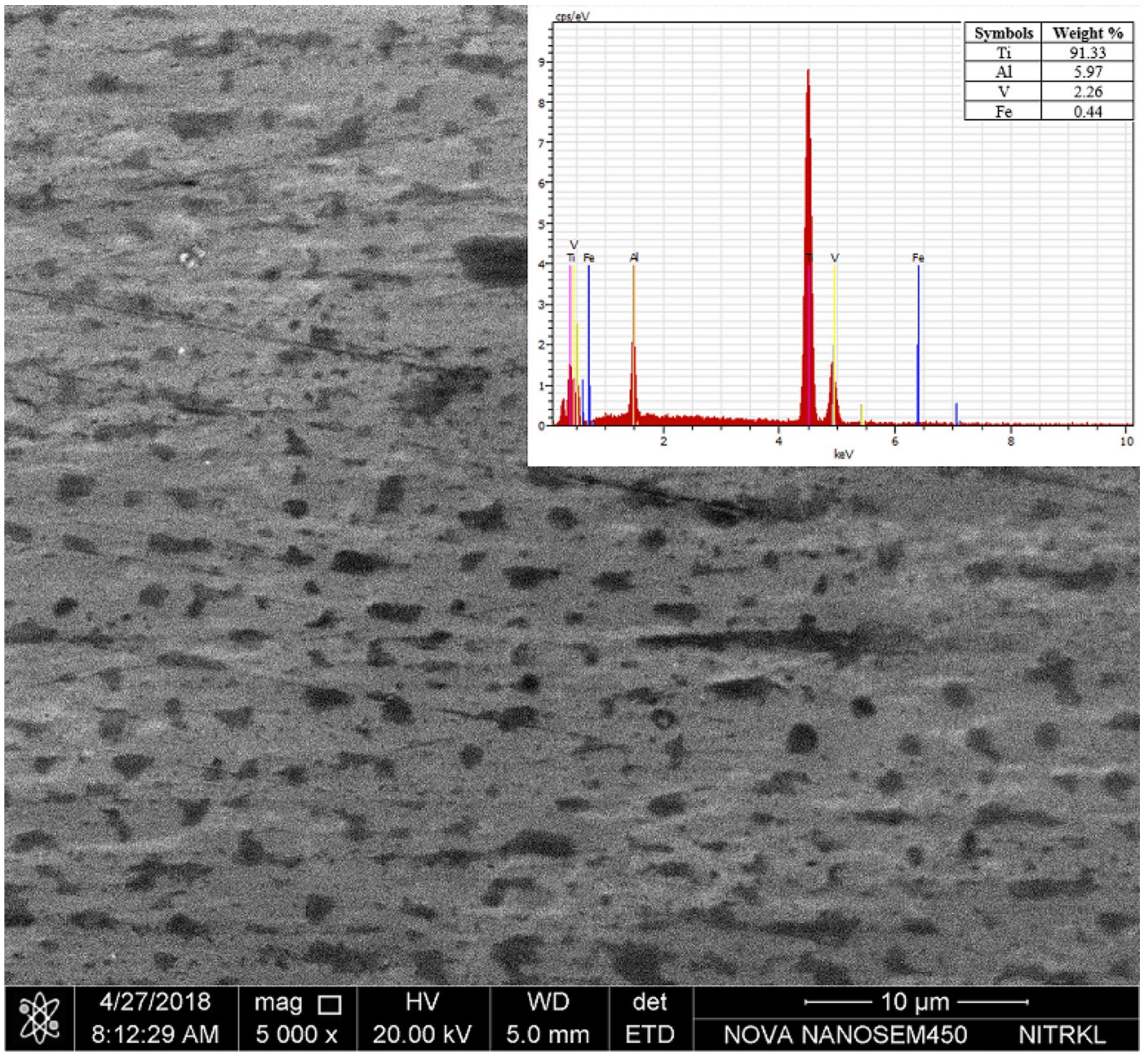

Fig. 3 FESEM-EDS graph for work piece 1 (Ti6Al4V as received)

pulsed millisecond (ms) Nd:YAG laser machine developed at Raja Ramanna Centre for Advanced Technology (RRCAT), Indore, India. Pulsed Nd:YAG laser system with 250 W average power, 5 kW maximum peak power, 1–20 ms pulse duration and 1–100 Hz repetition rate has been used for micro-drilling process. Laser beam has been delivered through a 200 µm-core diameter and 0.22 numerical aperture (NA) silica–silica fiber. Argon gas is used as an assistant gas to protect the laser lens from any damage and flushing of molten material during laser beam micro-drilling process. Schematic layout for the present experimentation (laser drilling process) has been shown in Fig. 4. Here, offset distance of 3 mm has been considered. The process parameters

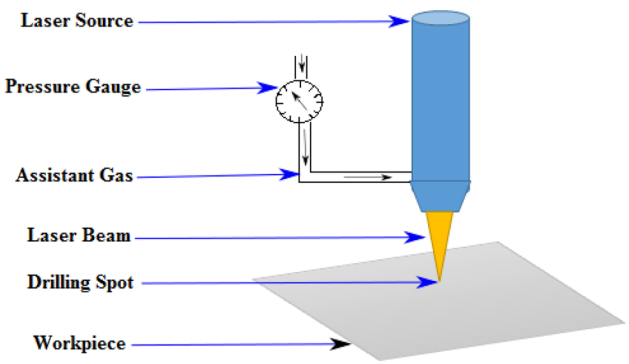

Fig. 4 Schematic layout of the laser drilling process

Table 2 Laser drilling setup and the parametric levels

Settings		Ranges		
Focal position		0 (on the surface) (fixed)		
Gas flow rate (lpm)		10		
Average Power (W)		250		
Offset distance (mm)		3		
Work piece (for laser drilling)		Ti6Al4V and AISI 316		
Control parameters	Symbols	Levels		
		1	2	3
Laser beam micro-drilling parameters and their levels				
Pulse width (ms)	A	4	6	8
Current (A)	B	200	230	260
Pulse frequency (Hz)	C	1	4	7
Gas pressure (Argon gas) (bar)	D	4	6	8

considered after extensive literature survey [40–43] and control parameters available with the laser drilling setup in RRCAT, Indore.

The process parameters considered for the laser beam micro-drilling process are current, pulse frequency, pulse width and gas pressure and each at three levels (low, medium and high) as shown in Table 2. The laser beam drilling setup and their parametric levels are discussed in Table 2 below. If all the probable factor combinations would have been considered, it would require 3^4 experimental runs. To determine the influence of process parameters on performance measures with less number of experimental runs, Taguchi method has been employed. Taguchi's L_{27} orthogonal array is used to design the experimental matrix (Tables 3 and 4) and each experimental trial is repeated twice.

4 Results and discussion

Laser beam micro drilling is a thermal ablation process in which high-intensity energy beam is focused at a point. Laser guided beam helps in melting and evaporation of molten material from the focused zone on the work piece. The remaining molten material from the machined area is flushed away using assistant gas pressure. The improper flushing of molten materials may cause expelled materials to be deposited on the surface area of the drilled holes leading to several irregularities in terms of circularity at entry and exit, heat-affected zone, spatter area and taper. Drilled samples are tested under optical and scanning electron microscope (SEM) to determine the quality characteristics such as circularity at entry (Cent), circularity at exit (Cexit), heat-affected zone (HAZ), spatter area (SA) and taper of laser drilled micro holes. The experiments have been conducted according to experimental layout using Taguchi's L_{27} orthogonal array. The experimental conditions are shown in Tables 3 and 4 for AISI 316 and Ti6Al4V, respectively. Each experiment is repeated twice and average value is noted down. The normalized values of performance measures under each treatment combination are shown in Tables 3 and 4. The normalization of performance measures is carried out using Eqs. 1 and 2. Let x_{ij} be the experimental response value for jth response in ith trial and $x_{\min}$ and $x_{\max}$ are the maximum and minimum experimental response for jth response.

Normalization:

$$\text{Lower the better} = \frac{x_{\max} - x_{ij}}{x_{\max} - x_{\min}}, \tag{1}$$

$$\text{Higher the better} = \frac{x_{ij} - x_{i\min}}{x_{\max} - x_{\min}}. \tag{2}$$

"Larger the better" characteristic is preferred for performance measures like circularity at entry and exit, whereas "Lower the better" characteristic is recommended for heat affected zone, spatter area and taper.

Improper flushing of molten materials may cause expelled material to be deposited on the surface area of the drilled holes, known as spatter area. Spatter area is calculated as shown in Fig. 5. The surface area of the total molten material deposited on the surface of each hole, known as spatter area, is calculated for both the materials.

For the calculation of circularity at entry, circularity at exit and HAZ, spatter deposition on the surface of the laser drilled samples are removed by emery polishing with paper III grade 1/0 (Kohinoor Products, India). To calculate the circularity of the hole and its dimensions, the drilled samples are taken under optical microscope (Carl Zeiss, GERMANY) and analyzed. The circularity is defined as the ratio of minimum diameter (D_{minimum}) to maximum diameter (D_{maximum}) of Ferret's hole diameter as expressed in Eq. 3. Figure 6a and b indicates the calculation of circularity of laser drilled holes for AISI 316 and Ti6Al4V, respectively, using Ferret's hole diameter concept:

$$\text{Circularity} = \frac{D_{\text{minimum}}}{D_{\text{maximum}}}. \tag{3}$$

Figure 7a and b indicates the pictographic representation of laser drilled holes at entry and exit, respectively, for AISI 316 for experiment number 5. Similarly, Fig. 7c

Table 3 Experimental layout and normalized performance measures (AISI 316)

Exp. no.	A	B	C	D	Cent	Cexit	HAZ	SA	Taper
1	1	1	1	1	0.7112	0.6491	0.7941	0.6757	0.7963
2	1	1	2	2	0.8534	0.7518	0.9000	0.4039	0.3930
3	1	1	3	3	0.7091	0.7118	0.8306	0.5147	0.2528
4	1	2	1	2	0.2294	0.2203	0.6999	0.7696	0.7726
5	1	2	2	3	0.4923	0.4907	0.6440	0.6988	0.3665
6	1	2	3	1	0.7263	0.6445	0.6598	0.4967	0.1143
7	1	3	1	3	0.1000	0.1000	0.4144	0.9000	0.8001
8	1	3	2	1	0.6021	0.5218	0.3683	0.7008	0.6484
9	1	3	3	2	0.6993	0.6496	0.4222	0.6921	0.2705
10	2	1	1	2	0.5779	0.5265	0.7694	0.6354	0.7781
11	2	1	2	3	0.7655	0.7007	0.7451	0.4860	0.3891
12	2	1	3	1	0.8946	0.9000	0.7245	0.2511	0.1017
13	2	2	1	3	0.1490	0.3095	0.5758	0.8827	0.7714
14	2	2	2	1	0.9000	0.7866	0.5633	0.2975	0.6468
15	2	2	3	2	0.6993	0.6282	0.5330	0.4649	0.2451
16	2	3	1	1	0.4911	0.3983	0.3271	0.7732	0.9028
17	2	3	2	2	0.5538	0.3774	0.2650	0.7280	0.6324
18	2	3	3	3	0.5254	0.7592	0.2354	0.7086	0.3317
19	3	1	1	3	0.5375	0.4684	0.6311	0.7438	0.7709
20	3	1	2	1	0.8811	0.8707	0.6168	0.1000	0.6705
21	3	1	3	2	0.7545	0.6803	0.6484	0.3999	0.1999
22	3	2	1	1	0.6096	0.5214	0.3986	0.6437	0.8757
23	3	2	2	2	0.7382	0.6566	0.4170	0.5153	0.6335
24	3	2	3	3	0.8149	0.7718	0.4680	0.4673	0.2754
25	3	3	1	2	0.3063	0.2645	0.1000	0.8269	0.8890
26	3	3	2	3	0.5242	0.4930	0.1378	0.7468	0.6120
27	3	3	3	1	0.6524	0.8717	0.1217	0.5409	0.2749

Cent circularity at entry, *Cexit* circularity at exit, *HAZ* heat-affected zone, *SA* spatter area

and d indicates the pictographic representation of laser drilled holes at entry and exit, respectively, for Ti6Al4V for experiment number 5. From the figures, difference of hole diameter at entry and exit for both the work pieces can be clearly observed. This indicates that the presence of taper on laser drilled micro-holes. Taper of the drilled holes is calculated by Eq. 4 stated below:

$$\text{Taper} = \frac{(\text{Diameter at entry}) - (\text{Diameter at exit})}{2 \times (\text{thickness of workpiece})}. \quad (4)$$

After analysis of geometrical features of the laser drilled hole, the samples are cloth polished and etched to reveal the HAZ of each hole for both the materials. Scanning electron microscope (SEM) (JEOL JSM-6480LV, USA) has been used to calculate the HAZ. In laser beam drilling process, a high amount of thermal energy is developed during machining operation. The thermal energy leads to change in microstructure near the drilled holes, known as heat affected zone (HAZ). Figure 8a and b indicates the HAZ for AISI 316 and Ti6Al4V work piece, respectively. While comparing Fig. 8a with Fig. 8b, it is observed that HAZ value is higher for Ti6Al4V work piece as compared to AISI 316 work piece under identical experimental conditions (experiment number 5). Higher value of HAZ is observed in case of titanium alloy work piece. It may be attributed to low thermal conductivity of titanium alloys as compared to stainless steel. As heat is not properly dissipated and localized near the machining zone, it results in higher HAZ value at parametric setting at 4 ms of pulse width, 230 A of laser current, 4 Hz of pulse frequency and 8 bar gas pressure (experiment number 5). Figure 8c indicates formation of burrs and surface erosion in drilled hole for AISI 316 workpiece. The formation of burrs may occur due to insufficient flushing pressure. Surface cracking may

Table 4 Experimental layout and normalized performance measures (Ti6Al4V)

Exp. no.	A	B	C	D	Cent	Cexit	HAZ	SA	Taper
1	1	1	1	1	0.2962	0.2853	0.8449	0.5690	0.5917
2	1	1	2	2	0.4962	0.9000	0.8629	0.6933	0.6345
3	1	1	3	3	0.9000	0.6937	0.9000	0.8465	0.7379
4	1	2	1	2	0.1731	0.1674	0.7782	0.6529	0.8434
5	1	2	2	3	0.3923	0.3779	0.6921	0.7377	0.8414
6	1	2	3	1	0.6192	0.5926	0.6607	0.9000	0.1697
7	1	3	1	3	0.1000	0.1000	0.7115	0.6948	0.9000
8	1	3	2	1	0.4269	0.4116	0.2933	0.7871	0.3166
9	1	3	3	2	0.5231	0.5042	0.3131	0.8516	0.3848
10	2	1	1	2	0.3192	0.3105	0.8103	0.1550	0.6814
11	2	1	2	3	0.5423	0.5211	0.7844	0.3558	0.5331
12	2	1	3	1	0.7692	0.7358	0.6754	0.4559	0.2269
13	2	2	1	3	0.2154	0.2137	0.6037	0.3245	0.6448
14	2	2	2	1	0.5462	0.5253	0.5100	0.3314	0.3345
15	2	2	3	2	0.6423	0.6179	0.6037	0.4795	0.3110
16	2	3	1	1	0.2538	0.2474	0.3468	0.2793	0.7338
17	2	3	2	2	0.4538	0.4368	0.2772	0.3751	0.5917
18	2	3	3	3	0.5692	0.5463	0.2360	0.5809	0.5917
19	3	1	1	3	0.3346	0.3232	0.5357	0.1000	0.5593
20	3	1	2	1	0.6654	0.6389	0.4870	0.2817	0.3634
21	3	1	3	2	0.7828	0.7490	0.6631	0.4505	0.3387
22	3	2	1	1	0.4706	0.4514	0.4331	0.2841	0.4563
23	3	2	2	2	0.6123	0.5869	0.5078	0.3807	0.4236
24	3	2	3	3	0.6548	0.6300	0.4758	0.5635	0.4722
25	3	3	1	2	0.3762	0.3639	0.3473	0.3527	0.7314
26	3	3	2	3	0.5416	0.5204	0.2817	0.5033	0.6380
27	3	3	3	1	0.6588	0.6338	0.5650	0.4685	0.4876

Cent circularity at entry, *Cexit* circularity at exit, *HAZ* heat-affected zone, *SA* spatter area

be due to prolonged heating effect on the material. Figure 8d indicates development of micro-cracks in the HAZ of the micro-drilled holes for Ti6Al4V alloy. As thermal conductivity of Ti6Al4V is low, it leads to localization of heat near the machined area resulting in development of thermal stress near the drilled region. The thermal stresses cause formation of micro-cracks (distortion) near the drilled zone. It is clearly observed that the hole quality differs for both the materials during laser beam drilling of AISI 316 and Ti6Al4V under same experimental parametric setup (experiment number 5).

The development of micro-cracks in the machining zone of Ti6Al4V is an important issue that needs to be addressed. The present study is further extended to analyze the formation micro-cracks near the drilling zone. Figure 9 helps to understand the parametric effect on formation of micro-cracks near the drilled area of Ti6Al4V alloy. Figure 9 indicates that thermal input energy (due to factor A and B), pulse frequency (C) and assistant gas pressure (D) have huge contribution in development of micro-cracks near the drilled holes. It is clearly observed that drilled hole with less thermal input energy, less crack intensity is observed as compared to drilled holes with higher thermal input energy. The development of micro-cracks and their propagation occur due to several reasons like development of thermal stress in machined zone, gas pressure, increment of pulse frequency and fracture toughness. Increase in thermal input energy causes increase in thermal stress within the machined region. When thermal stress exceeds the limit of ultimate strength of the workpiece, it results in development of cracks in the machined zone. Increase in pulse frequency leads to reduction of pulse-off-time and escalation of rate of heat input during laser beam drilling process. If thermal conductivity of the material is less and the developed thermal energy is

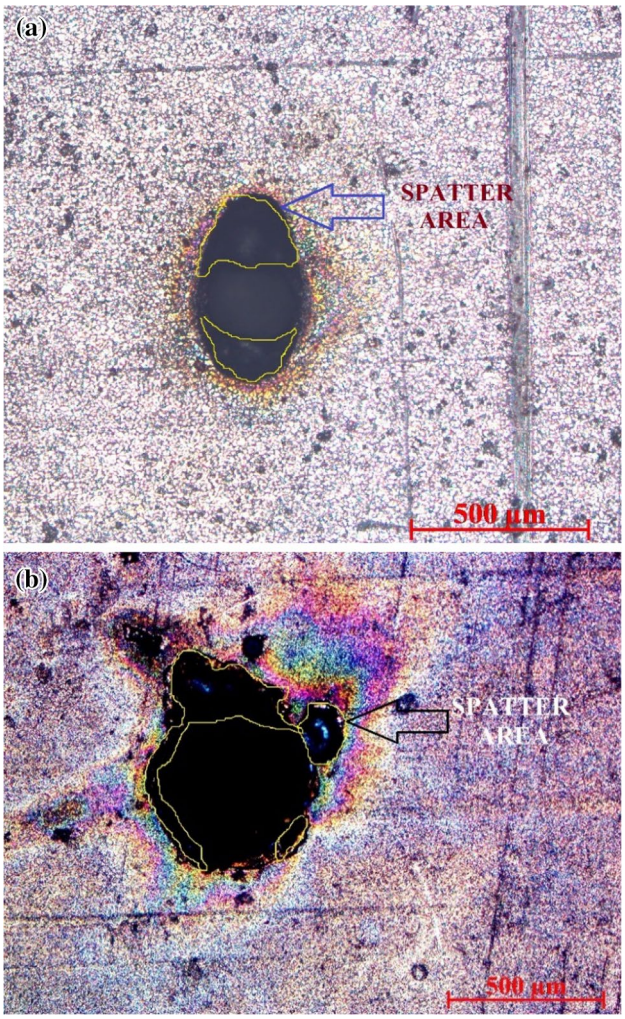

Fig. 5 Deposition of spatter on surface area of the drilled holes for **a** AISI 316 and **b** Ti6Al4V

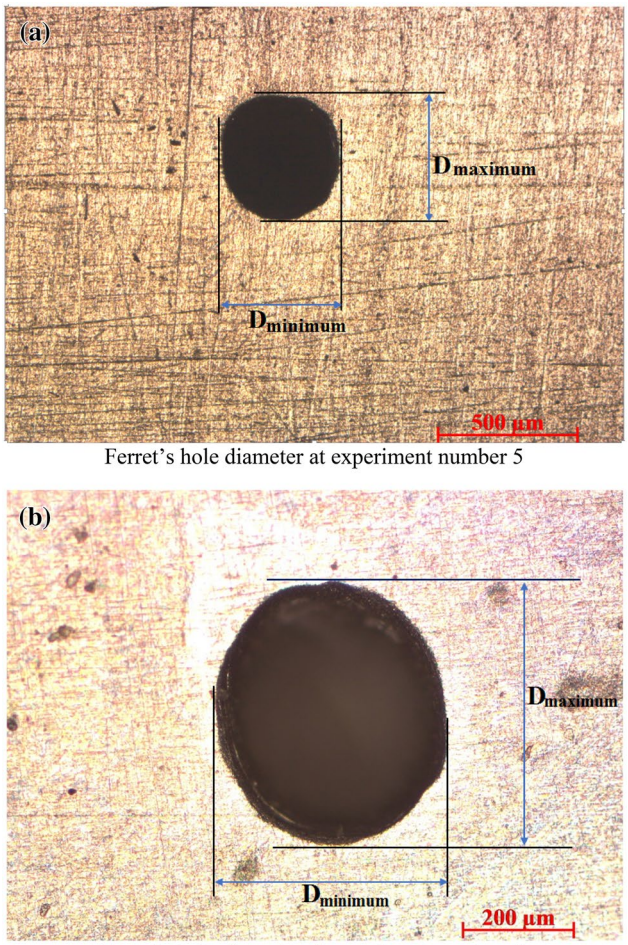

Fig. 6 **a** Ferret hole diameter for AISI 316 drilled sample and **b** Ferret's hole diameter for Ti6Al4V drilled sample

not easily dissipated (or concentrated near the machining zone), it may lead to distortion near machined zone in form of cracks. Increase in gas pressure leads to increase in cooling rate. Change in sudden temperature difference leads to increase the crack intensity [44].

4.1 Prediction of hole quality through ANFIS

To predict the performance measures such as circularity at entry (Cent), circularity at exit (Cexit), heat affected zone (HAZ), spatter area (SA) and taper for laser beam drilling on AISI 316 and Ti6Al4V, adaptive neuro fuzzy inference system (ANFIS) toolbox available with MATLAB 2017b has been used. Sugeno model has been used for the analysis (Fig. 10). The ANFIS analysis has been performed in two phases, namely training and testing. 70% experimental data (20 sets of data) considered for training and remaining 30% (7 data) which are not included in training of the network taken for testing of the developed network. The four input parameters and Gaussian type membership function (gaussmf) are considered for prediction model in ANFIS. Subtractive clustering has been selected for generating the fuzzy inference system (FIS). In training phase, the model become stable after three iterations where 0.01 is the error tolerance value (20 experimental data are taken). This states that the model is well developed. Now to check the adequacy of the developed model, the testing of the model has been performed using seven experimental data from experiment numbers 21 to 27 (Tables 6, 7). The proposed steps for

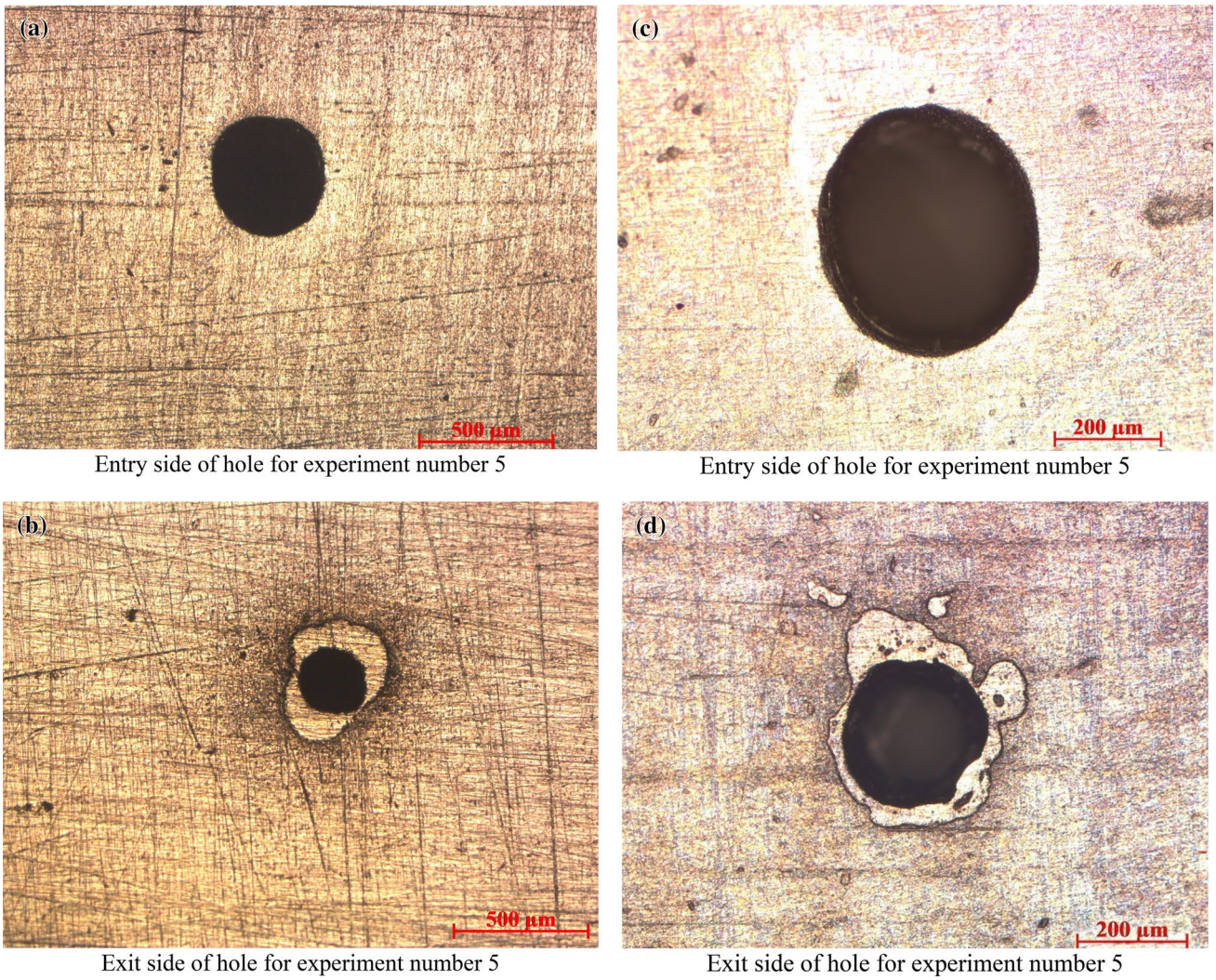

Fig. 7 Laser drilled hole images for experimental run number 5 **a** and **b** for AISI 316 and **c** and **d** for Ti6Al4V work piece

the ANFIS model can be easily observed in Figs. 10, 11, 12, 13, and 14. Figure 10 indicates the proposed Sugeno model for the fuzzy system (for AISI 316 laser drilled samples), Fig. 11 shows the developed clustering rules for the membership functions and Fig. 12 indicates the developed adaptive network for the ANFIS model (for AISI 316 laser drilled samples). Figures 13 and 14 show the comparative graph plot between the predicted data (training and testing) and actual data (for AISI 316 laser drilled samples). Figures 12 and 13 also represent the obtained training and testing errors, respectively, for HAZ of AISI 316 laser drilled sample. Similarly, the analysis is performed for other performance measures for both the work pieces for each performance measures and they are depicted in Tables 6 and 7 for AISI 316 and Ti6Al4V samples, respectively.

4.2 Prediction of hole quality through MGGP

To predict the performance measures for laser beam drilling on AISI 316 and Ti6Al4V, multi-gene genetic programming (MGGP) has been used using MATLAB 2017b. The code is available in the open source [45]. The experimented data have been divided into two parts viz. training data and testing data. 70% experimental data (20 sets of data) is considered for training and remaining 30% (7 data) which not contributed in training of the network taken for testing of

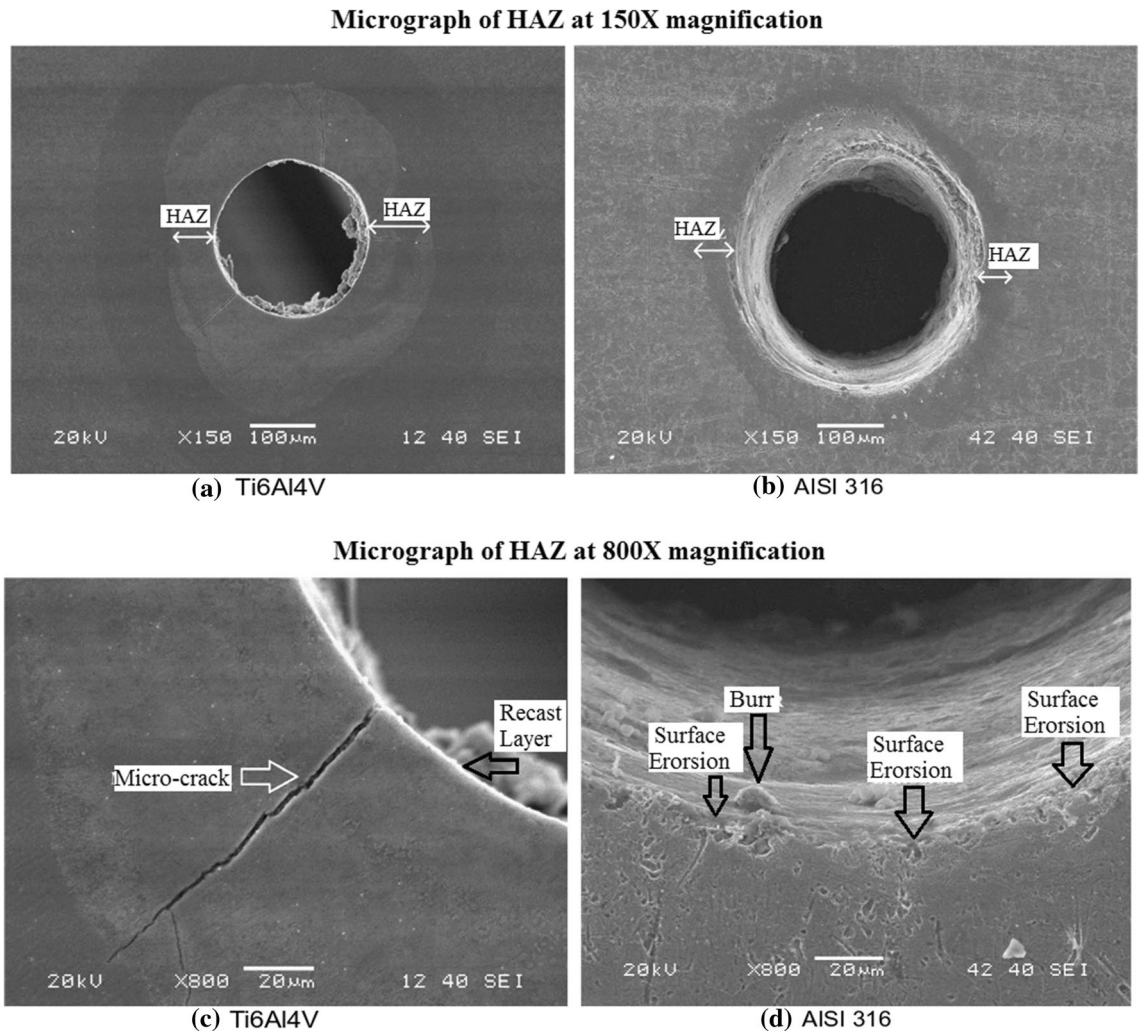

Fig. 8 HAZ for AISI 316 and Ti6Al4V laser drilled hole at experimental run number 5

the proposed methodology. The control parameters and their settings are the predominant factor in instigating MGGP algorithm effectively. Trial and error methodology has been adapted to decide the parametric settings (Table 5). The function set consists of broader set of elements so as to evolve variety of non-linear forms of mathematical models. The values of population size and number of generations fairly depend on the complexity of the data. Based on literature review by Garg and Tai [17], the population size and number of generations should be fairly large for data of higher complexity so as to find the models with minimum error. Maximum number of genes and maximum depth of the gene influence the size and the number of models to be searched in the global space. The maximum number of genes and maximum depth of gene are chosen at eight and six, respectively. GPTIPS-2 [45] software is used for the implementation of MGGP algorithm. The preeminent multi gene genetic programming (MGGP) model is selected based on minimum root mean square error (RMSE) obtained from testing data trails as shown in Tables 8 and 9.

The detailed analysis for MGGP model has been presented through Figs. 15, 16, and 17. Figure 15 indicates the multi-gene regression model for the population size in proposed MGGP model. Figure 16 indicates the residual plots for the training and testing data for HAZ (AISI 316 sample). The residual plot suggests the adequacy of the proposed MGGP model. Figure 17 shows the comparative graph plots between the predicted data and experimental data in training and testing phase of the MGGP algorithm. The root mean square error (RMSE) of 0.06531 and comparative plot suggests the adequacy of the proposed model for the analysis. Similarly, the analysis is performed for other performance measures for both the work pieces depicted in Tables 6 and 7 for AISI 316 and Ti6Al4V samples, respectively.

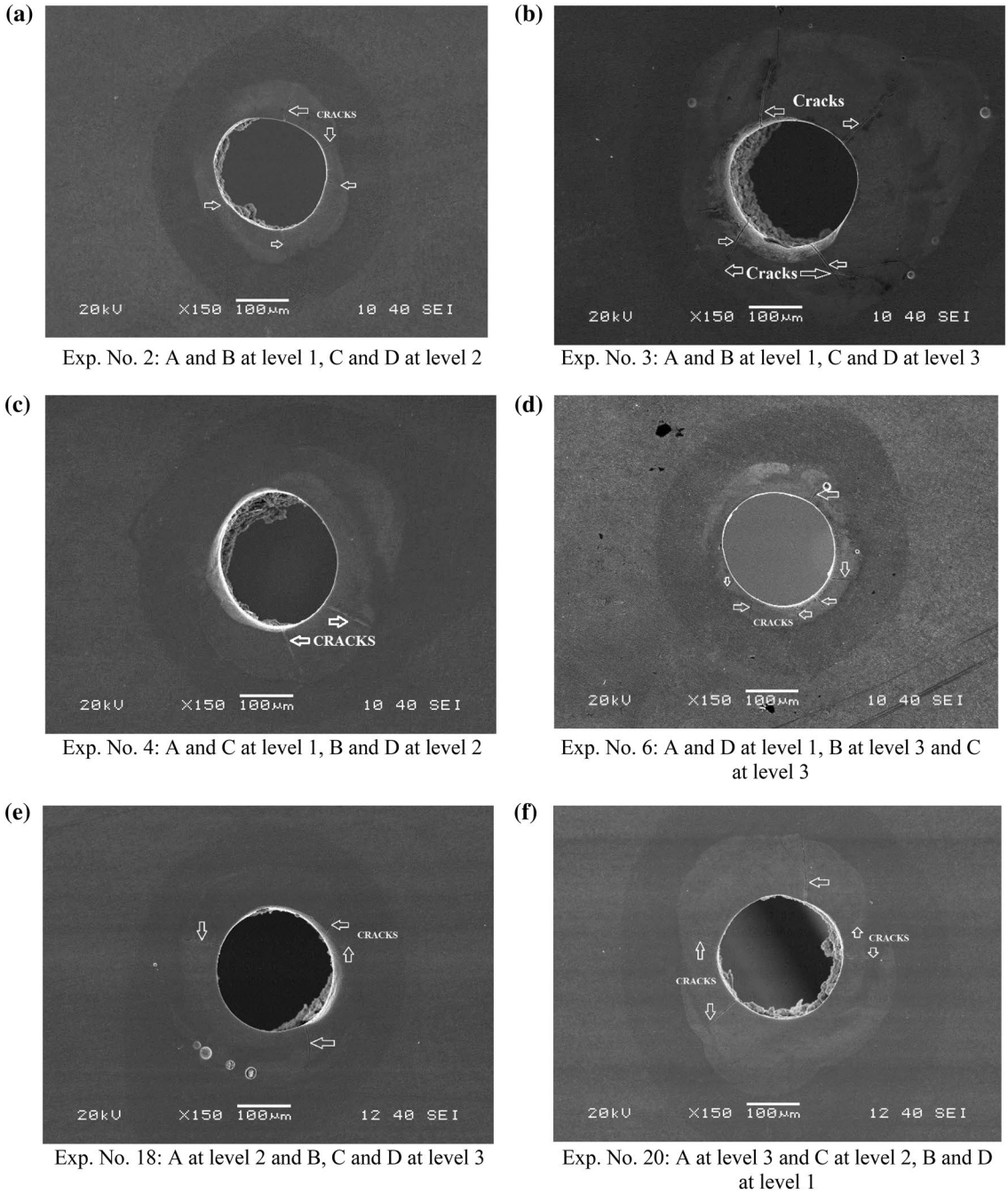

Exp. No. 2: A and B at level 1, C and D at level 2

Exp. No. 3: A and B at level 1, C and D at level 3

Exp. No. 4: A and C at level 1, B and D at level 2

Exp. No. 6: A and D at level 1, B at level 3 and C at level 3

Exp. No. 18: A at level 2 and B, C and D at level 3

Exp. No. 20: A at level 3 and C at level 2, B and D at level 1

Fig. 9 Formation of micro-cracks on Ti6Al4V laser drilled samples

To analyze the effectiveness of both the proposed predictive models, a comparative analysis is made in Tables 6 and 7 for stainless steel (AISI 316) and titanium alloy (Ti6Al4V) work pieces. From the study, it is observed that both the techniques are quite adequate in predicting the performance measures in training phase. To determine the adequacy of the models during testing phase, comparative graphs for testing data are shown in Figs. 18 and 19 for AISI 316 and Ti6Al4V, respectively. It is noted that MGGP model shows minimum root mean square error (RMSE) as compared to ANFIS model for the chosen performance measures (Tables 8 and 9). The results suggest that MGGP is potentially superior and adequate in predicting the performance measures for laser beam micro-drilling process.

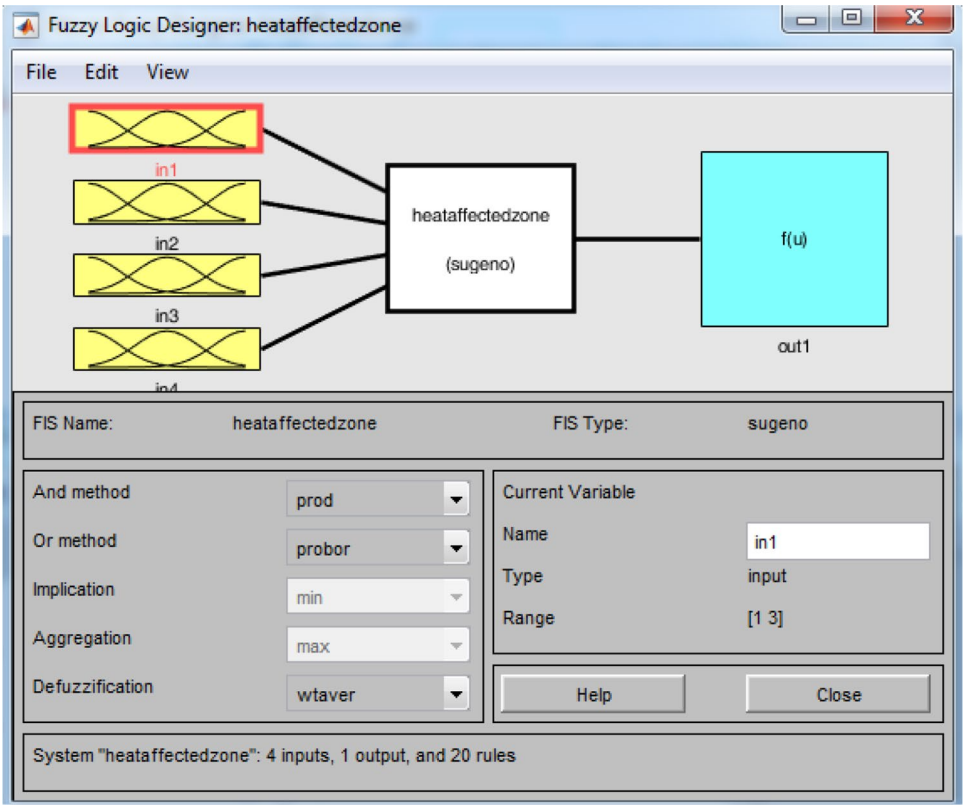

Fig. 10 Layout of ANFIS Sugeno model for HAZ (AISI 316)

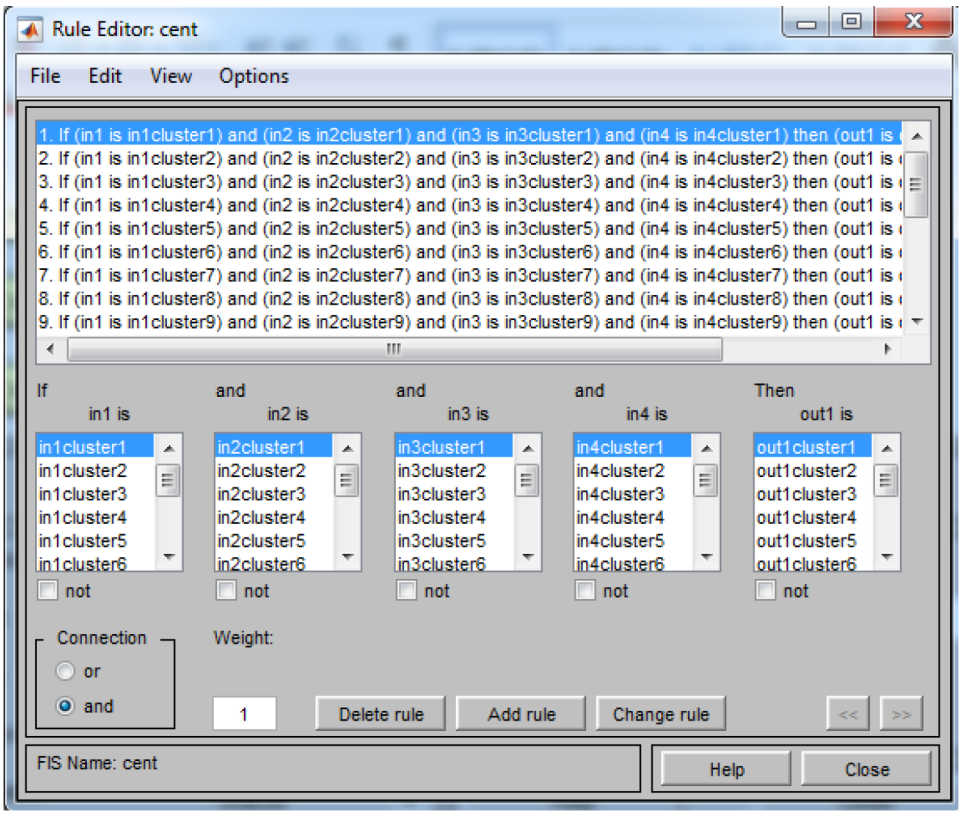

Fig. 11 Fuzzy rule for the proposed ANFIS model (AISI 316)

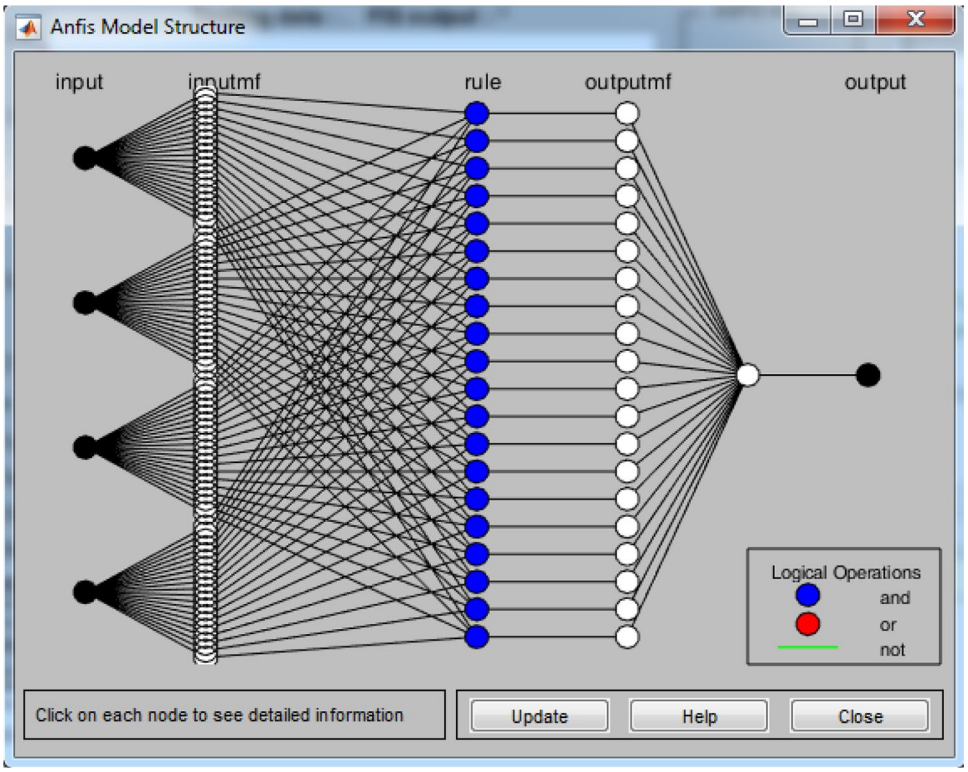

Fig. 12 Network model structure for the proposed ANFIS model (AISI 316)

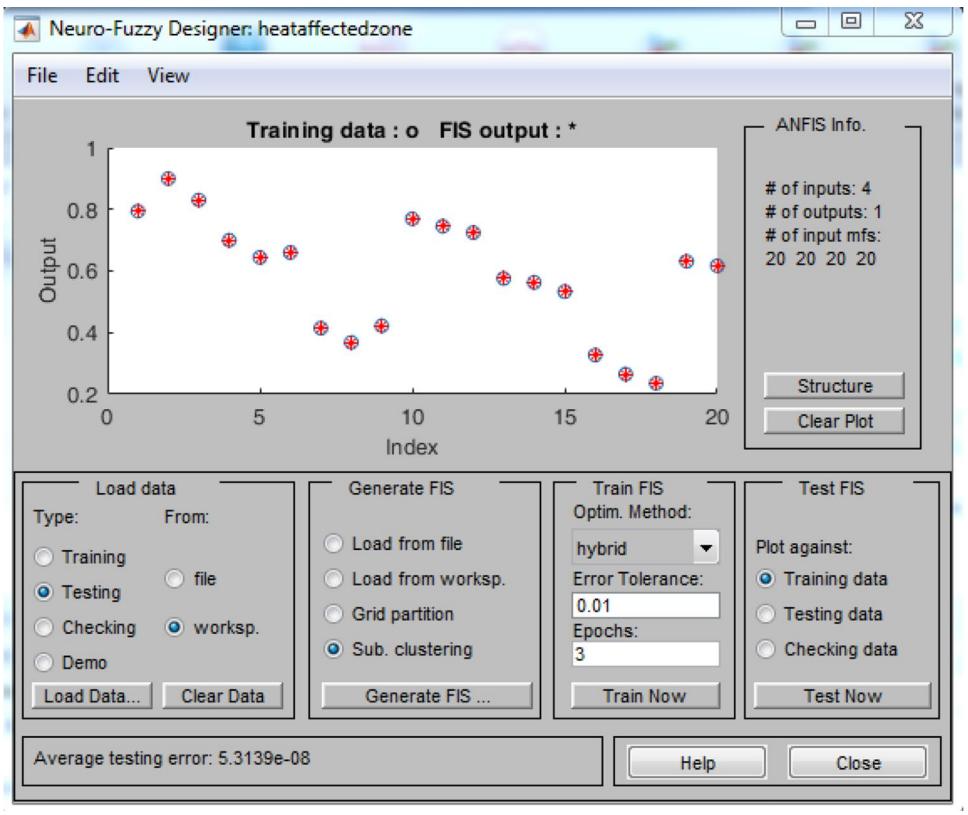

Fig. 13 Representation of training experimental data vs training predicted data and obtained average error for the training data for HAZ (AISI 316)

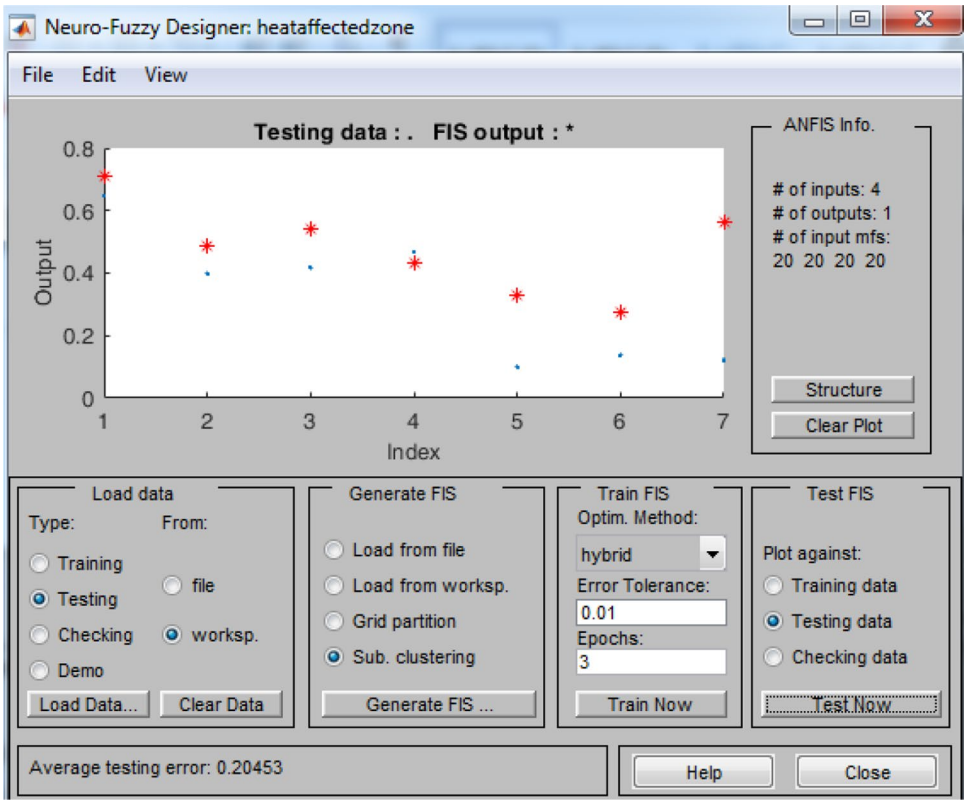

Fig. 14 Representation of testing experimental data vs testing predicted data and obtained average error for the training data for HAZ (AISI 316)

Table 5 Parameter settings for proposed MGGP model

Parameters	Ranges
Population size	270
Timeout	10 s
Iterations	3
Tournament size	25
Maximum genes	6

5 Conclusion

In the present study, laser beam drilling on AISI 316 and Ti6Al4V of 0.45 mm thickness has been performed using millisecond pulsed Nd:YAG laser using Taguchi's experimental plan to collect experimental data. The study is intended to propose a predictive model using artificial intelligence techniques. After extensive literature review, it is observed that ANFIS and MGGP are two potential competing artificial techniques for predicting the performance measures in laser material processing techniques [13, 16, 29]. A comparative study has been performed to analyze the adequacy of the ANFIS and MGGP models for predicting the performance measures of the laser drilled holes. Laser drilling on AISI 316 and Ti6Al4V has been performed under identical experimental conditions (same parametric settings). Following are the outcomes of the present investigation:

- Laser beam micro-drilling on AISI 316 and Ti6Al4V is possible under identical experimental parametric settings.
- Under identical machining conditions (for example experiment number 5), AISI 316 resists thermal shocks although micro-cracks are observed for few machining conditions. However, micro-cracks on the drilled surface for all the machining condition when Ti6Al4V work piece is used. The development of micro-cracks in Ti6Al4V work piece may be attributed to low thermal conductivity of the material and fracture toughness

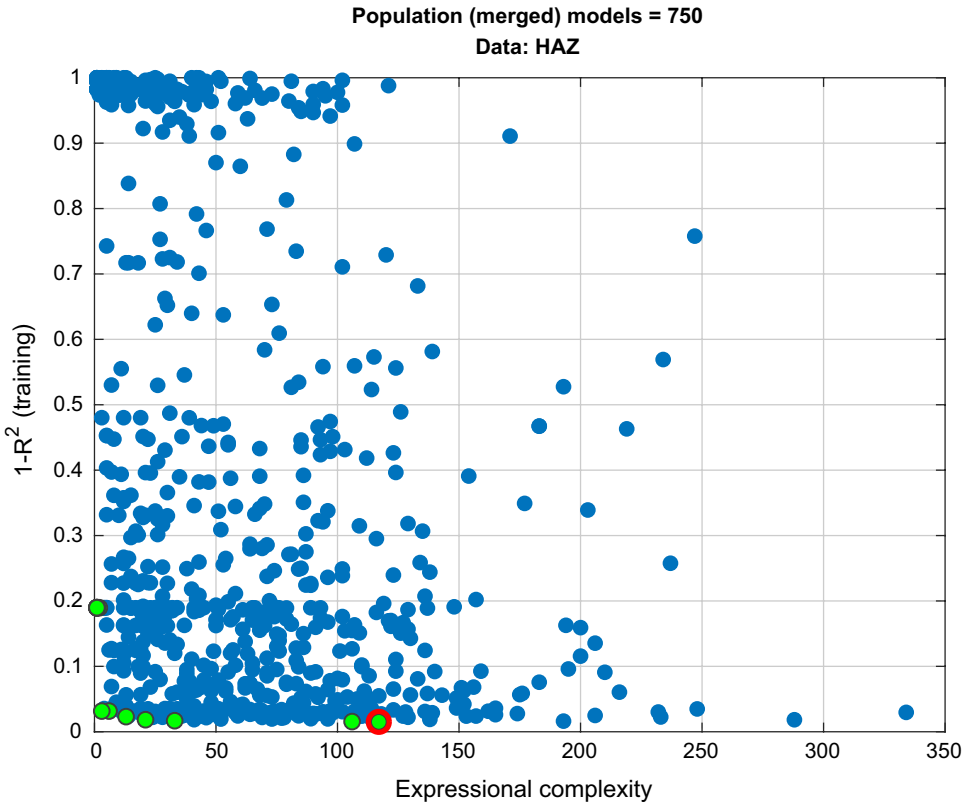

Fig. 15 Multi-gene regression for population size in MGGP for HAZ (AISI 316)

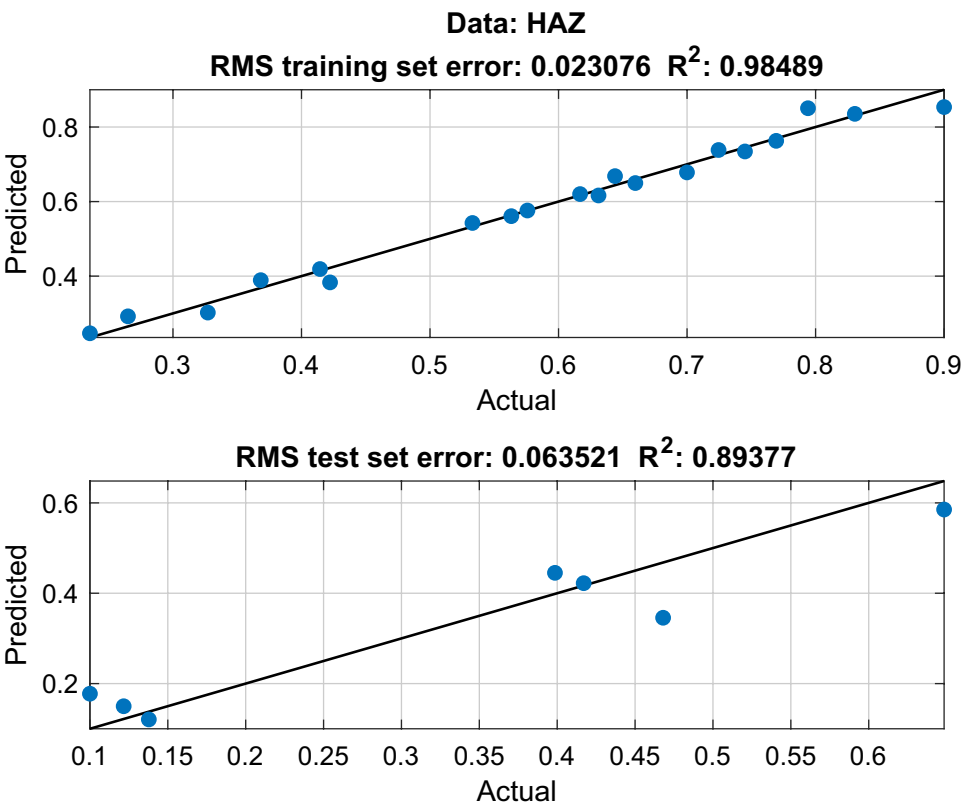

Fig. 16 Residual plots of MGGP model for HAZ (AISI 316)

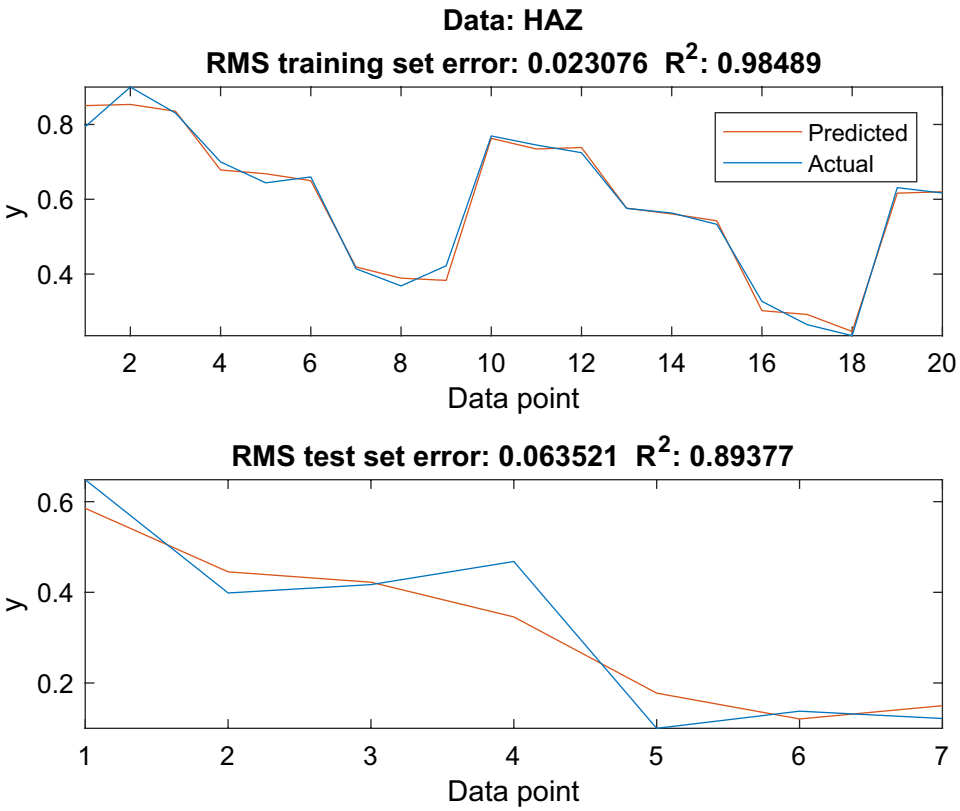

Fig. 17 Representation of predicted data vs experimental data of MGGP model (training and testing) for HAZ (AISI 316)

and development of high thermal stress in the machining zone exceeding the ultimate tensile strength.

- While comparing the hole quality for both materials, AISI 316 has low circularity, high spatter area and development of surface erosion of the hole. This may be due to prolonged heating effect of the materials.
- From the study, it can be concluded that both the artificial techniques such as ANFIS and MGGP are quite adequate in predicting the performance measures for laser drilling of AISI 316 and Ti6Al4V in training phase. To determine the superior prediction capability among the two proposed models, a comparative study for predicting the testing data has been performed.
- It is noted that MGGP model shows minimum root mean square error (RMSE) as compared to ANFIS model for the performance measures. The results suggest that MGGP has more potentiality and adequacy in predicting the performance measures for laser beam microdrilling process. It can be concluded that MGGP models have higher prediction accuracy as compared to ANFIS model.

Table 6 Predicted performance measures using ANFIS and MGGP (AISI 316)

Exp. no.	Cent		Cexit		HAZ		SA		Taper		Data sets
	MGGP	ANFIS	MGGP	ANFIS	MGGP	ANFIS	MGGP	ANFIS	MGGP	ANFIS	
1	0.6704	0.7112	0.6168	0.6491	0.8504	0.7941	0.6234	0.6757	0.7260	0.7963	Training data
2	0.8070	0.8534	0.6927	0.7518	0.8535	0.9000	0.4659	0.4039	0.4358	0.3930	
3	0.7588	0.7091	0.7158	0.7119	0.8353	0.8306	0.5000	0.5147	0.1611	0.2528	
4	0.2991	0.2294	0.2948	0.2203	0.6783	0.6999	0.8012	0.7696	0.7672	0.7726	
5	0.4683	0.4923	0.5231	0.4907	0.6683	0.6440	0.6491	0.6988	0.5102	0.3665	
6	0.7003	0.7263	0.7623	0.6445	0.6497	0.6598	0.4937	0.4967	0.1258	0.1143	
7	0.1509	0.1000	0.1587	0.1000	0.4190	0.4144	0.9790	0.9000	0.8086	0.8001	
8	0.6978	0.6021	0.5276	0.5218	0.3892	0.3683	0.6052	0.7008	0.5677	0.6484	
9	0.6171	0.6993	0.4868	0.6496	0.3832	0.4222	0.6823	0.6921	0.2467	0.2705	
10	0.5567	0.5779	0.4812	0.5265	0.7629	0.7694	0.6368	0.6354	0.7613	0.7781	
11	0.7259	0.7655	0.6940	0.7007	0.7344	0.7451	0.4726	0.4860	0.4625	0.3891	
12	0.9579	0.8946	0.9172	0.9000	0.7384	0.7245	0.2336	0.2511	0.1617	0.1017	
13	0.1854	0.1490	0.2975	0.3095	0.5761	0.5758	0.8781	0.8827	0.7608	0.7715	
14	0.7323	0.9000	0.7139	0.7866	0.5609	0.5633	0.4160	0.2975	0.6034	0.6468	
15	0.6516	0.6993	0.6555	0.6282	0.5426	0.5330	0.4947	0.4649	0.2406	0.2451	
16	0.4799	0.4911	0.3474	0.3983	0.3022	0.3271	0.7518	0.7732	0.9680	0.9028	
17	0.6166	0.5539	0.4349	0.3774	0.2921	0.2650	0.6672	0.7280	0.6362	0.6324	
18	0.5684	0.5254	0.7674	0.7592	0.2467	0.2354	0.7559	0.7087	0.3198	0.3317	
19	0.4536	0.5375	0.4775	0.4684	0.6164	0.6311	0.7108	0.7438	0.7197	0.7709	
20	0.9000	0.8811	0.9003	0.8707	0.6201	0.6168	0.1063	0.1000	0.6718	0.6705	
21	0.9198	0.9368	0.7881	0.9125	0.5853	0.7105	0.1604	0.2951	0.2543	0.3874	Testing data
22	0.5250	0.7330	0.5023	0.6620	0.4452	0.4853	0.5259	0.3740	0.8936	0.7084	
23	0.6617	0.8213	0.5941	0.7270	0.4223	0.5410	0.4468	0.4090	0.6497	0.5971	
24	0.6135	0.6688	0.7768	0.7402	0.3457	0.4320	0.5169	0.6179	0.2785	0.3071	
25	0.3768	0.5650	0.2295	0.4247	0.1776	0.3294	0.8505	0.8242	0.8812	0.8521	
26	0.5460	0.5774	0.6167	0.5926	0.1207	0.2739	0.7873	0.7766	0.6277	0.5384	
27	0.7780	0.9006	0.6641	0.7561	0.1499	0.5617	0.5554	0.5754	0.4364	0.6273	

ANFIS adaptive neuro-fuzzy inference system, *MGGP* multi gene genetic programming, *Cent* circularity at entry, *Cexit* circularity at exit, *HAZ* heat-affected zone, *SA* spatter area

Table 7 Predicted performance measures using ANFIS and MGGP (Ti6Al4V)

Exp. no.	Cent		Cexit		HAZ		SA		Taper		Data sets
	MGGP	ANFIS	MGGP	ANFIS	MGGP	ANFIS	MGGP	ANFIS	MGGP	ANFIS	
1	0.3428	0.2962	0.3721	0.2853	0.6348	0.8449	0.5848	0.5690	0.8739	0.5917	Training data
2	0.5066	0.4962	0.6677	0.9000	0.5752	0.8629	0.6821	0.6933	0.8707	0.6345	
3	0.8525	0.9000	0.7287	0.6937	0.7386	0.9000	0.8541	0.8465	0.8720	0.7379	
4	0.2041	0.1731	0.1952	0.1674	0.7592	0.7782	0.5999	0.6529	0.7531	0.8435	
5	0.3730	0.3923	0.4832	0.3779	0.8231	0.6921	0.7719	0.7377	0.7951	0.8414	
6	0.6173	0.6192	0.5871	0.5926	0.1532	0.6607	0.8725	0.9000	0.6263	0.1697	
7	0.1030	0.1000	0.0314	0.1000	0.9077	0.7115	0.6898	0.6948	0.6289	0.9000	
8	0.3625	0.4269	0.4295	0.4116	0.3976	0.2933	0.7903	0.7871	0.3791	0.3166	
9	0.5466	0.5231	0.4819	0.5042	0.4202	0.3131	0.8876	0.8516	0.3213	0.3848	
10	0.3304	0.3192	0.3437	0.3105	0.6941	0.8103	0.1815	0.1550	0.7400	0.6814	
11	0.5265	0.5423	0.6410	0.5211	0.5900	0.7844	0.3535	0.3558	0.7529	0.5331	
12	0.7980	0.7692	0.6983	0.7358	0.1443	0.6754	0.4541	0.4559	0.6883	0.2269	
13	0.1917	0.2154	0.1840	0.2137	0.7287	0.6037	0.2714	0.3245	0.6822	0.6448	
14	0.4784	0.5462	0.5356	0.5253	0.4043	0.5100	0.3719	0.3314	0.5157	0.3345	
15	0.6897	0.6423	0.5914	0.6179	0.3243	0.6037	0.4692	0.4795	0.5395	0.3110	
16	0.3279	0.2539	0.2144	0.2474	0.6642	0.3469	0.2897	0.2793	0.2967	0.7338	
17	0.3824	0.4539	0.5030	0.4368	0.5382	0.2772	0.3871	0.3751	0.2750	0.5917	
18	0.6190	0.5692	0.5454	0.5463	0.5819	0.2360	0.5591	0.5809	0.2453	0.5917	
19	0.3389	0.3346	0.3056	0.3232	0.5062	0.5357	0.1406	0.1000	0.5600	0.5593	
20	0.6470	0.6654	0.6105	0.6390	0.4060	0.4870	0.2411	0.2817	0.5111	0.3635	
21	0.8798	0.7828	0.6697	0.7490	0.2090	0.6631	0.3384	0.4505	0.5262	0.3387	Testing data
22	0.4374	0.4706	0.2487	0.4514	0.6814	0.4331	0.1589	0.2841	0.3313	0.4563	
23	0.5134	0.6123	0.5408	0.5869	0.4529	0.5078	0.2563	0.3807	0.3755	0.4236	
24	0.7715	0.6548	0.5925	0.6300	0.3164	0.4759	0.4283	0.5635	0.4313	0.4722	
25	0.3363	0.3762	0.3162	0.3639	0.6969	0.3473	0.1741	0.3527	0.1547	0.7314	
26	0.4174	0.5416	0.5948	0.5204	0.5093	0.2817	0.3461	0.5033	0.1655	0.6380	
27	0.5740	0.6589	0.7454	0.6338	0.1524	0.5650	0.4466	0.4685	0.1672	0.4876	

Cent circularity at entry, *Cexit* circularity at exit, *HAZ* heat-affected zone, *SA* spatter area

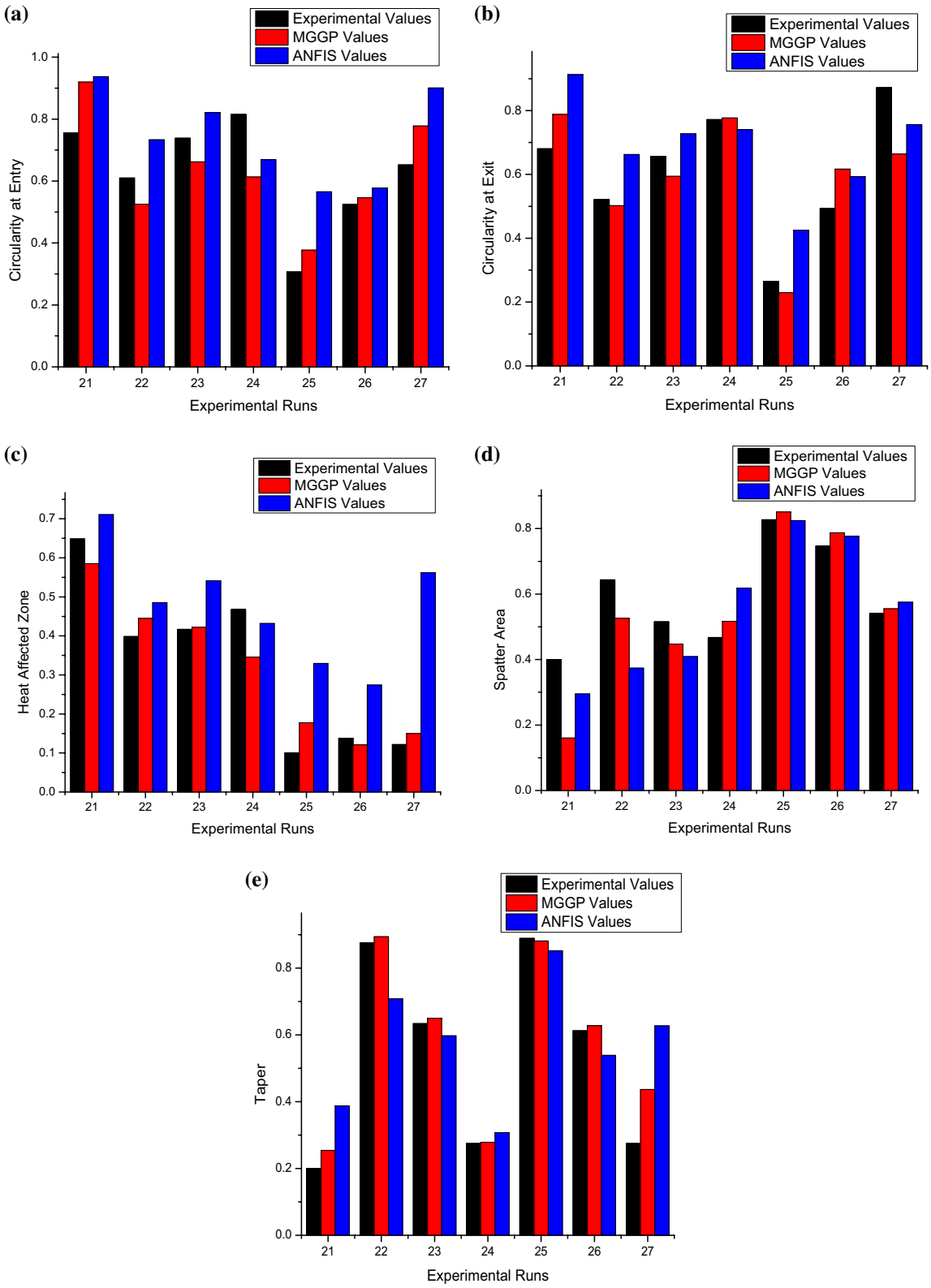

Fig. 18 Comparative graphs for experimental data and predicted testing data for ANFIS and MGGP (AISI 316 workpiece)

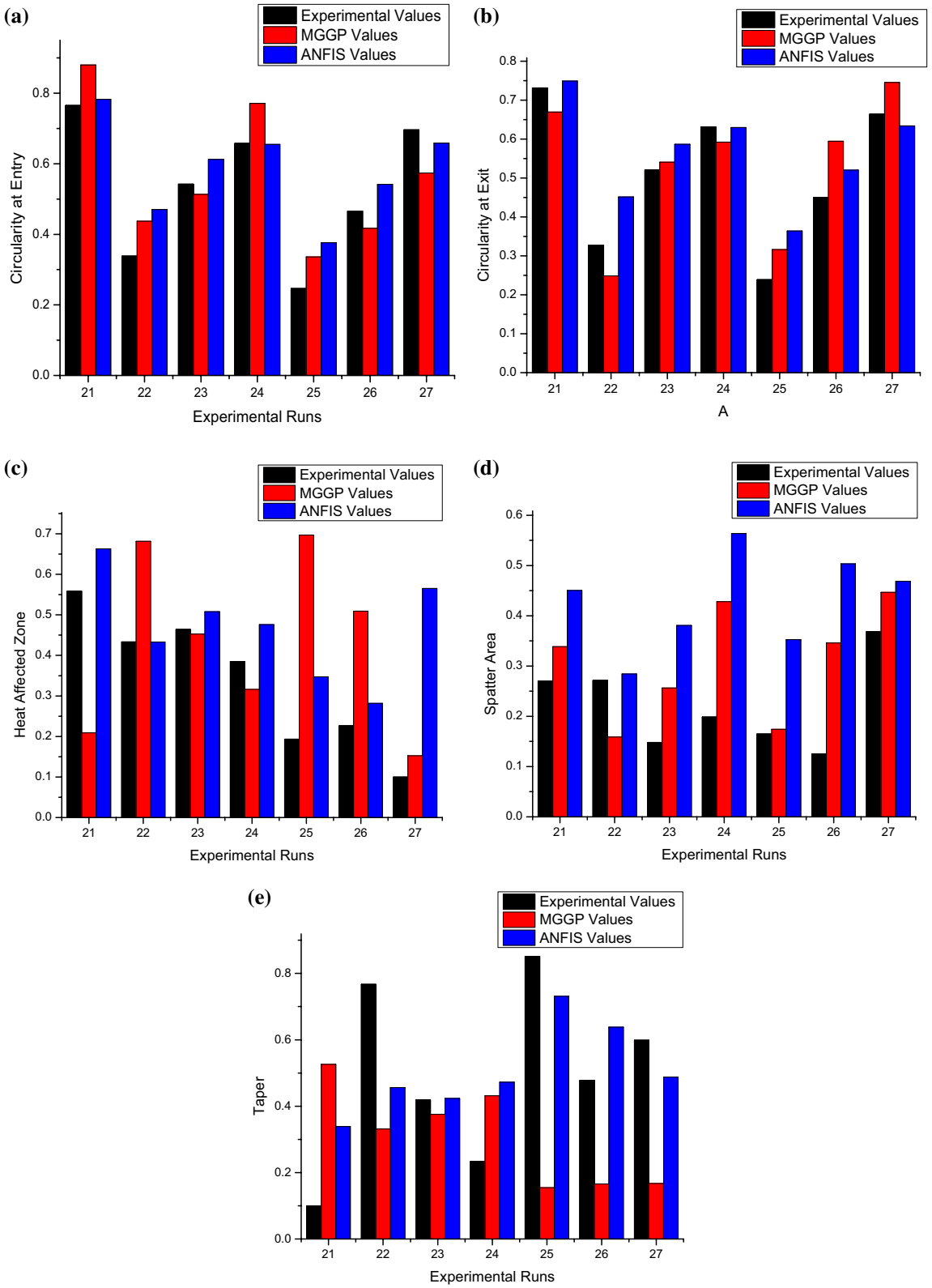

Fig. 19 Comparative graphs for experimental data and predicted testing data for ANFIS and MGGP (Ti6Al4V work piece)

Table 8 Root mean square error (RMSE) for testing data using ANFIS and MGGP (AISI 316 workpiece)

Performance measures	AISI 316	
	MGGP	ANFIS
Circularity at entry	0.1024	0.1724
Circularity at exit	0.1039	0.1356
Heat affected zone	0.0635	0.2045
Spatter area	0.1074	0.1308
Taper	0.0955	0.2045

Table 9 Root mean square error (RMSE) for testing data using ANFIS and MGGP (Ti6Al4V work piece)

Performance measures	Ti6Al4V	
	MGGP	ANFIS
Circularity at entry	0.0404	0.0817
Circularity at exit	0.0807	0.0771
Heat-affected zone	0.0758	0.1942
Spatter area	0.1399	0.2417
Taper	0.1834	0.1937

References

1. Shen H, Jiang J, Feng D, Xing C, Zhao X, Xiao P (2019) Environmental Effect on the Crack Behavior of Yttria-Stabilized Zirconia during Laser Drilling. J Manuf Sci Eng 141(5):054501
2. Adelmann B, Hellmann R (2015) Rapid micro hole laser drilling in ceramic substrates using single mode fiber laser. J Mater Process Technol 221:80–86
3. Bharatish A, Murthy HN, Anand B, Madhusoodana CD, Praveena GS, Krishna M (2013) Characterization of hole circularity and heat affected zone in pulsed CO_2 laser drilling of alumina ceramics. Opt Laser Technol 53:22–32
4. Dubey AK, Yadava V (2008) Experimental study of Nd: YAG laser beam machining-An overview. J Mater Process Technol 195(1–3):15–26
5. Casalino G (2018) Computational intelligence for smart laser materials processing. Opt Laser Technol 100:165–175
6. Hajihassani M, Kalatehjari R, Marto A, Mohamad H, Khosrotash M (2019) 3D prediction of tunneling-induced ground movements based on a hybrid ANN and empirical methods. Eng Comput. https://doi.org/10.1007/s00366-018-00699-5
7. Parandoush P, Hossain A (2014) A review of modeling and simulation of laser beam machining. Int J Mach Tools Manuf 85:135–145
8. Vijayaraghavan V, Garg A, Wong CH, Tai K, Mahapatra SS (2014) Measurement of properties of graphene sheets subjected to drilling operation using computer simulation. Measurement 50:50–62
9. Sibalija TV, Petronic SZ, Majstorovic VD, Prokic-Cvetkovic R, Milosavljevic A (2011) Multi-response design of Nd: YAG laser drilling of Ni-based superalloy sheets using Taguchi's quality loss function, multivariate statistical methods and artificial intelligence. Int J Adv Manuf Technol 54(5–8):537–552
10. Bello O, Holzmann J, Yaqoob T, Teodoriu C (2015) Application of artificial intelligence methods in drilling system design and operations: a review of the state of the art. J Artif Intell Soft Comput Res 5(2):121–139
11. Gill SS, Singh J (2010) An Adaptive Neuro-Fuzzy Inference System modeling for material removal rate in stationary ultrasonic drilling of sillimanite ceramic. Expert Syst Appl 37(8):5590–5598
12. Pérez JA, González M, Dopico D (2010) Adaptive neurofuzzy ANFIS modeling of laser surface treatments. Neural Comput Appl 19(1):85–90
13. Garg A, Tai K, Vijayaraghavan V, Singru PM (2014) Mathematical modelling of burr height of the drilling process using a statistical-based multi-gene genetic programming approach. Int J Adv Manuf Technol 73(1–4):113–126
14. Abhishek K, Panda BN, Datta S, Mahapatra SS (2014) Comparing predictability of genetic programming and ANFIS on drilling performance modeling for GFRP composites. Procedia Mater Sci 6:544–550
15. Abidin NWZ, Ab Rashid MFF, Mohamed NMZN (2019) A review of multi-holes drilling path optimization using soft computing approaches. Arch Comput Methods Eng 26(1):107–118
16. Desai CK, Shaikh A (2012) Prediction of depth of cut for single-pass laser micro-milling process using semi-analytical, ANN and GP approaches. Int J Adv Manuf Technol 60(9–12):865–882
17. Garg A, Tai K (2014) Stepwise approach for the evolution of generalized genetic programming model in prediction of surface finish of the turning process. Adv Eng Softw 78:16–27
18. Arnaiz-González Á, Fernández-Valdivielso A, Bustillo A, de Lacalle LNL (2016) Using artificial neural networks for the prediction of dimensional error on inclined surfaces manufactured by ball-end milling. Int J Adv Manuf Technol 83(5–8):847–859
19. Khandelwal M, Faradonbeh RS, Monjezi M, Armaghani DJ, Majid MZBA, Yagiz S (2017) Function development for appraising brittleness of intact rocks using genetic programming and nonlinear multiple regression models. Eng Comput 33(1):13–21
20. Asiltürk I, Çunkaş M (2011) Modeling and prediction of surface roughness in turning operations using artificial neural network and multiple regression method. Expert Syst Appl 38(5):5826–5832
21. Laouissi A, Yallese MA, Belbah A, Belhadi S, Haddad A (2019) Investigation, modeling, and optimization of cutting parameters in turning of gray cast iron using coated and uncoated silicon nitride ceramic tools. Based on ANN, RSM, and GA optimization. Int J Adv Manuf Technol 101(1–4):523–548
22. Bustillo A, Correa M (2012) Using artificial intelligence to predict surface roughness in deep drilling of steel components. J Intell Manuf 23(5):1893–1902
23. Gholami A, Bonakdari H, Ebtehaj I, Mohammadian M, Gharabaghi B, Khodashenas SR (2018) Uncertainty analysis of intelligent model of hybrid genetic algorithm and particle swarm optimization with ANFIS to predict threshold bank profile shape based on digital laser approach sensing. Measurement 121:294–303
24. Petković D, Nikolić V, Milovančević M, Lazov L (2016) Estimation of the most influential factors on the laser cutting process heat affected zone (HAZ) by adaptive neuro-fuzzy technique. Infrared Phys Technol 77:12–15
25. Abdulshahed AM, Longstaff AP, Fletcher S (2015) The application of ANFIS prediction models for thermal error compensation on CNC machine tools. Appl Soft Comput 27:158–168
26. Abdulshahed AM, Longstaff AP, Fletcher S, Myers A (2015) Thermal error modelling of machine tools based on ANFIS with fuzzy c-means clustering using a thermal imaging camera. Appl Math Model 39(7):1837–1852
27. Al-Ghamdi K, Taylan O (2015) A comparative study on modelling material removal rate by ANFIS and polynomial methods in electrical discharge machining process. Comput Ind Eng 79:27–41
28. Sohrabpoor H (2016) Analysis of laser powder deposition parameters: ANFIS modeling and ICA optimization. Optik-Int J Light Electron Opt 127(8):4031–4038

29. Sohrabpoor H (2017) Perspective of applying adaptive neuro fuzzy inference system (ANFIS) in laser cladding of graphene-metal alloys. J Nanotechnol 4:017
30. Sahu M, Khatua KK, Mahapatra SS (2011) A neural network approach for prediction of discharge in straight compound open channel flow. Flow Meas Instrum 22(5):438–446
31. Koza JR (1995) Survey of genetic algorithms and genetic programming. In: Wescon conference record. Western periodicals company, pp 589–594. https://doi.org/10.1109/WESCON.1995.485447
32. Koza JR (1994) Genetic programming II, vol 17. MIT press, Cambridge
33. Koza JR, Koza JR (1992) Genetic programming: on the programming of computers by means of natural selection, vol 1. MIT press, Cambridge
34. Kaydani H, Mohebbi A, Eftekhari M (2014) Permeability estimation in heterogeneous oil reservoirs by multi-gene genetic programming algorithm. J Petrol Sci Eng 123:201–206
35. Sharma N, Kumar K, Raj T, Kumar V (2019) Porosity exploration of SMA by Taguchi, regression analysis and genetic programming. J Intell Manuf 30(1):139–146
36. Panda B, Shankhwar K, Garg A, Savalani MM (2019) Evaluation of genetic programming-based models for simulating bead dimensions in wire and arc additive manufacturing. J Intell Manuf 30(2):809–820
37. Kök M, Kanca E, Eyercioğlu Ö (2011) Prediction of surface roughness in abrasive waterjet machining of particle reinforced MMCs using genetic expression programming. Int J Adv Manuf Technol 55(9–12):955–968
38. Garg A, Lam JSL (2015) Improving environmental sustainability by formulation of generalized power consumption models using an ensemble based multi-gene genetic programming approach. J Clean Prod 102:246–263
39. Brezocnik M, Kovacic M, Ficko M (2004) Prediction of surface roughness with genetic programming. J Mater Process Technol 157:28–36
40. Bandyopadhyay S, Sundar JS, Sundararajan G, Joshi SV (2002) Geometrical features and metallurgical characteristics of Nd: YAG laser drilled holes in thick IN718 and Ti–6Al–4V sheets. J Mater Process Technol 127(1):83–95
41. Bharatish A, Murthy HN, Anand B, Madhusoodana CD, Praveena GS, Krishna M (2013) Characterization of hole circularity and heat affected zone in pulsed CO_2 laser drilling of alumina ceramics. Opt Laser Technol 53:22–32
42. Olsen FO, Alting L (1995) Pulsed laser materials processing, ND-YAG versus CO_2 lasers. CIRP Ann 44(1):141–145
43. Ghany KA, Newishy M (2005) Cutting of 1.2 mm thick austenitic stainless steel sheet using pulsed and CW Nd: YAG laser. J Mater Process Technol 168(3):438–447
44. Chatterjee S, Mahapatra SS, Sahu AK, Bhardwaj VK, Choubey A, Upadhyay BN, Bindra KS (2017) Experimental and parametric evaluation of quality characteristics in Nd: YAG laser micro-drilling of Ti6Al4V and AISI 316. In: ASME 2017 gas turbine India conference. American Society of Mechanical Engineers Digital Collection. https://doi.org/10.1115/GTINDIA2017-4679
45. Searson DP (2015) GPTIPS 2: an open-source software platform for symbolic data mining. In: Gandomi A, Alavi A, Ryan C (eds) Handbook of genetic programming applications. Springer, Cham. https://doi.org/10.1007/978-3-319-20883-1_22